Preparation of novel alkylated ruthenium .alpha.-diimine complexes: reactivity toward carbon monoxide and phosphines

Marco J. A. Kraakman, Kees Vrieze, Huub Kooijman, and Anthony L. Spek

Organometallics, **1992**, 11 (11), 3760-3773• DOI: 10.1021/om00059a046 • Publication Date (Web): 01 May 2002

Preparation of Novel Alkylated Ruthenium α-Diimine Complexes: Reactivity toward Carbon Monoxide and Phosphines

Marco J. A. Kraakman and Kees Vrieze*

Anorganisch Chemisch Laboratorium, J. H. van't Hoff Instituut, Universiteit van Amsterdam, Nieuwe Achtergracht 166, 1018 WV Amsterdam, The Netherlands

Huub Kooijman and Anthony L. Spek

Bijvoet Center for Biomolecular Research, Vakgroep Kristal- en Structuurchemie, RijksUniversiteit Utrecht, Padualaan 8, 3584 CH Utrecht, The Netherlands

Received June 9, 1992

$Ru_2(CO)_5(^iPr\text{-}DAB)$ (1) reacts with MeI at room temperature to give $Ru_2(Me)(I)(CO)_4(^iPr\text{-}DAB)$ (**2a**), and a single-crystal X-ray structure determination of **2a** has been obtained. Crystals of **2a** are orthorhombic, space group *Pbca*, with unit-cell dimensions a = 16.2510 (10) Å, b = 13.2660 (10) Å, and c = 17.2410 (10) Å. The molecular structure consists of a $Ru(Me)(CO)_2$ fragment and a $Ru(CO)_2$ fragment, held together by an iodide bridge and a bridging α-diimine ligand. The DAB ligand is coordinated to the $Ru(Me)(CO)_2$ fragment via both nitrogen atoms and to the $Ru(CO)_2$ fragment via an η^2 coordination of both imine bonds. Treatment of **2a** with CO leads to substitution of the iodide bridge and the two coordinated imine bonds with the formation of $Ru(Me)(I)(CO)_2(^iPr\text{-}DAB)$ (**3a**) and $Ru(CO)_5$. This reaction, which is reversible, provides a new synthetic route for the preparation of monomeric methylated α-diimine complexes. Several other reaction routes for the formation of the complexes $Ru(X)(Y)(CO)_2$(α-diimine) (X = Me, Y = I, α-diimine = ^iPr-DAB (**3a**); X = Me, Y = I, α-diimine = ^iPr-Pyca (**3b**); X = Y = I, α-diimine = ^iPr-DAB (**3c**); X = Y = I, α-diimine = ^iPr-Pyca (**3d**); X = Cl, Y = benzyl, α-diimine = ^iPr-DAB (**3e**)) are presented. Treatment of **2a** with phosphines leads to substitution of only one coordinated imine bond, with the formation of $Ru_2(Me)(I)(CO)_4(PR_3)(^iPr\text{-}DAB)$ (PR_3 = PPh_3 (**4a**), PMe_2Ph (**4b**), $P(OMe)_3$ (**4c**)). A single-crystal X-ray structure determination of **4b** has been obtained, and crystal of **4b** are monoclinic, space group $P2_1/c$, with unit-cell dimensions a = 7.2030 (10) Å, b = 21.907 (2) Å, c = 16.813 (3) Å, and β = 94.352 (13)°. The molecular structure of **4b** consists of a $Ru(Me)(CO)_2$ fragment and a $Ru(CO)_2(PMe_2Ph)$ fragment which are bridged by an iodide atom and a 6e-donating $\sigma(N)$-$\mu_2(N')$-$\eta^2(C{=}N)$-bonded DAB ligand. Complexes **4a-c** easily lose a carbonyl ligand to form $Ru_2(Me)(I)(CO)_3(PR_3)(^iPr\text{-}DAB)$ (PR_3 = PPh_3 (**5a**), PMe_2Ph (**5b**), $P(OMe)_3$ (**5c**)), and this reaction is shown to be reversible. Upon treatment of **3a** with $Ru(CO)_4$ fragments complex **2a** is formed in good yield. Furthermore, reaction of **3a** with $Fe(CO)_4$ fragments leads to the formation of the heteronuclear complex $FeRu(Me)(I)(CO)_4(^iPr\text{-}DAB)$ (**2b**). In the presence of traces of water $HFeRu(Me)(CO)_5(^iPr\text{-}DAB)$ (**6**) is produced as a side product. A single-crystal X-ray structure determination of **6** has been obtained and crystals of **6** are monoclinic, space group $C2/c$, with unit-cell dimensions a = 18.102 (4) Å, b = 8.2761 (6) Å, c = 25.131 (4) Å, and β = 90.627 (16)°. As in **4b** the DAB ligand in **6** is $\sigma(N)$-$\mu_2(N')$-$\eta^2(C{=}N)$-coordinated to the bimetallic core, with the $\sigma(N)$ coordination to the Ru center and the $\eta^2(C{=}N)$ coordination to the Fe center. The hydride ligand of **6** was found to be bridging the metal-metal bond. Finally, the monomeric diiodide complex **3c** was reacted with $Ru(CO)_4$ fragments to form $Ru_2(I)_2(CO)_4(^iPr\text{-}DAB)$ (**7**).

Introduction

The chemistry of transition-metal complexes of α-diimines is dominated by the versatile coordination behavior of this type of organic ligand.[1] This versatility arises from the ability of the ligands to use both the lone pairs of the nitrogen atoms and the π systems of the two C=N bonds for coordination to a metal. The most frequently studied α-diimines are R-DAB,[2] R-Pyca,[2] and 2,2′-bipyridine (Figure 1). These ligands may donate up to a maximum of eight, six, and four electrons, respectively, whereas it has been noted that the π-accepting capacity decreases in this order.[1]

It has further been shown that (α-diimine)metal complexes may play an important role in homogeneous catalytic reactions. Fe(α-diimine) complexes, for instance, have been shown to be effective and selective catalysts for the cyclodimerization of 1,3-dienes;[3] Ru(α-diimine) complexes were used to catalyze the hydrogenation, the hydrosilation, and the isomerization of alkenes,[4] whereas in other cases α-diimine complexes of Ni,[5] Rh,[6] and Pd[7,8] were used as catalysts for oligomerization and hydrogenation processes.

Finally, in particular the compounds $M_2(CO)_6(L)$ (M_2 = Fe_2, FeRu, Ru_2; L = R-DAB, R-Pyca), containing 6e-donating bridging $\sigma(N)$-$\mu_2(N')$-$\eta^2(C{=}N')$-bonded α-diimine ligands, proved to be excellent starting materials for many stoichiometric reactions with small molecules such as H_2 and CO and with unsaturated substrates such as R-DAB, R-Pyca, carbodiimines (RN=C=NR), sulfines ($R_2C{=}S{=}O$), ketene ($H_2C{=}C{=}O$), allene ($H_2O{=}C{=}CH_2$), and alkynes (RC≡CR′), leading to an unusually rich chemistry involving C—C, C—H, C—N, and N—H coupling reactions.[1,9-12]

* To whom correspondence should be addressed.

(1) (a) van Koten, G.; Vrieze, K. *Adv. Organomet. Chem.* **1982**, *21*, 151. (b) Vrieze, K. *J. Organomet. Chem.* **1986**, *300*, 307. (c) van Koten, G.; Vrieze, K. *Recl. Trav. Chim. Pays-Bas* **1981**, *100*, 129. (d) Vrieze, K.; van Koten, G. *Inorg. Chim. Acta* **1985**, *100*, 79.

(2) The following abbreviations will be used throughout the text: R-DAB = 1,4-diaza-1,3-butadiene (RN=CHCH=NR); R-Pyca = pyridine-2-carbaldimine (C_5H_4N-2-CH=NR); IAE = 1,2-bis(alkylamino)-1,2-bis(alkylimino)ethane (RN=C(H)C(H)(NR)C(H)(NR)C(H)=NR); APE = 1,2-bis(alkylamido)-1,2-bis(2-pyridyl)ethane ((C_5H_4N-2)C(H)(NR)C(H)(NR)(2-C_5H_4N)).

(3) tom Dieck, H.; Kleinwächter, I.; Haupt, E. T. K. *J. Organomet. Chem.* **1987**, *321*, 237.

(4) Brockmann, M.; tom Dieck, H.; Klaus, J. *J. Organomet. Chem.* **1986**, *301*, 209.

(5) tom Dieck, H.; Lauer, A. M.; Stamp, L.; Diercks, R. *J. Mol. Catal.* **1986**, *35*, 317.

(6) tom Dieck, H.; Dietrich, J. *Angew. Chem., Int. Ed. Engl.* **1985**, *24*, 781.

(7) tom Dieck, H.; Munz, C.; Muller, C. *J. Organomet. Chem.* **1990**, *384*, 243.

(8) van Asselt, R.; Elsevier, C. J. *J. Mol. Catal.* **1991**, *65*, L13.

0276-7333/92/2311-3760$03.00/0

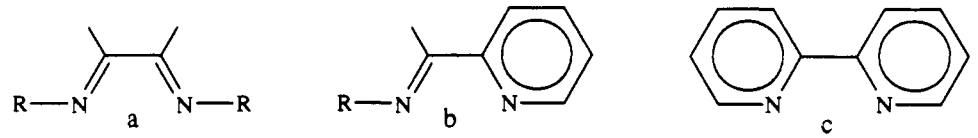

Figure 1. The most frequently studied α-diimine ligands R-DAB (a), R-Pyca (b), and bipyridine (c).

Treatment of $FeRu(CO)_6$(^{i}Pr-DAB) with molecular hydrogen led to an interesting trans-addition reaction,[13] whereas on the other hand treatment of $Ru_2(CO)_5$(^{i}Pr-DAB)[14] with molecular hydrogen gave rise to an oxidative-addition reaction, leading to the formation of $H_2Ru_2(CO)_5$(^{i}Pr-DAB).[10] The latter could be hydrogenated by further treatment with molecular hydrogen, but these reactions are not regioselective and are accompanied by C–H bond-making and -breaking processes.[15]

This difference in reactivity between the FeRu and Ru_2 complexes prompted us to extend the reactivity studies toward other oxidative addition reagents such as MeI, benzyl chloride, and I_2. The results of these investigations are presented here.

Experimental Section

1. Materials and Apparatus. ^{1}H and ^{13}C NMR spectra were recorded on a Bruker AC-100 and a Bruker AMX-300 spectrometer. IR spectra (ν(CO); 2200–1600 cm^{-1}) were measured on a Perkin-Elmer 283 spectrometer. Elemental analyses were carried out by the elemental analysis section of the Institute of Applied Chemistry TNO, Zeist, The Netherlands, or by Dornis und Kolbe Microanalytisches Laboratorium, Mülheim, Germany. All preparations were carried out under an atmosphere of purified nitrogen, using carefully dried solvents. Column chromatography was performed using silica gel (Kieselgel 60, Merck, 70–230 mesh ASTM, dried and activated before use) as the stationary phase. $Ru_3(CO)_{12}$ (Strem), PPh_3 (Merck), benzyl chloride (Ega-Chemie), iodomethane (Janssen), and carbon monoxide (Matheson) were used as commercially obtained. PMe_2Ph and $P(OMe)_3$ were obtained from Aldrich and distilled prior to use. Me_3NO was obtained from Aldrich and was dried before use by heating in vacuo. $Ru_2(CO)_6$(^{i}Pr-DAB)[11] and $Ru_2(CO)_4$(^{i}Pr-Pyca)$_2$[12] were prepared according to literature procedures. $Fe_2(CO)_9$ was prepared by a modified literature procedure.[16]

High-pressure NMR experiments were performed using a home-built apparatus consisting of a Ti/Al/V pressure head and a 10 mm external and 8.4 mm internal diameter sapphire NMR tube suitable for measurements up to 140 bar of gas pressure.[17] Both a Bruker AC-100 and a Bruker AMX-300 spectrometer were used to perform the high-pressure experiments.

2. Preparation of $Ru_2(Me)(I)(CO)_2$(^{i}Pr-DAB) (2a). A 255-mg amount of $Ru_2(CO)_6$(^{i}Pr-DAB)[11] (0.50 mmol) was dissolved in 40 mL of CH_2Cl_2 and treated with small portions of Me_3NO in CH_2Cl_2 until IR spectroscopy indicated that all the CO absorptions of the starting complex were replaced by those of $Ru_2(CO)_5$(^{i}Pr-DAB)[14] (1). Subsequently 2 mL of MeI was added to the mixture in one lot,[18] which rapidly caused the reaction mixture to turn into a yellow suspension.[19] The mixture was concentrated to 3 mL by evaporation of the solvent and purified by column chromatography. Elution with ligroin/CH_2Cl_2 (9/1) afforded a yellow fraction containing traces of $Ru_2(CO)_6$(^{i}Pr-DAB). The product $Ru_2(Me)(I)(CO)_4$(^{i}Pr-DAB) (2a) was obtained as an orange fraction by elution with ligroin/CH_2Cl_2 (7/3). Subsequent crystallization from hexane/CH_2Cl_2 at 20 °C yielded 2a in 70–75% yield (220 mg).

3. Synthesis of $Ru(Me)(I)(CO)_2$(^{i}Pr-DAB) (3a) from $Ru_2(Me)(I)(CO)_4$(^{i}Pr-DAB) (2a). A 200-mg amount of $Ru_2(Me)(I)(CO)_4$(^{i}Pr-DAB) (2a; 0.35 mmol was dissolved in 40 mL of hexane/CH_2Cl_2 (9/1) and stirred under an atmosphere of CO at room temperature. During the reaction the color of the reaction mixture changed from yellow/orange to red and the reaction was stopped when IR spectroscopy indicated that the conversion was complete (about 2 h). The reaction mixture, which now contained $Ru(Me)(I)(CO)_2$(^{i}Pr-DAB) (3a) together with $Ru(CO)_5$,[20] was then brought upon a column, and elution with ligroin/CH_2Cl_2 (9/1) afforded a yellow fraction containing $Ru(CO)_5$ and $Ru_3(CO)_{12}$. Elution with CH_2Cl_2 gave a red fraction containing 3a in more than 90% yield (140 mg).

4. Synthetic Routes for the Preparation of Complexes 3a–e. (a) Preparation of $Ru(Me)(I)(CO)_2$(^{i}Pr-DAB) (3a). A 320-mg amount of $Ru_3(CO)_{12}$ (0.5 mmol) and 420 mg of ^{i}Pr-DAB (3 mmol) were refluxed in hexane (60 mL) for 15 min. During this time the color of the mixture changed to dark red, indicating that the air-sensitive $Ru(CO)_3$(^{i}Pr-DAB) had been formed.[21,22] Subsequently 1.5 mL of MeI was added to the reaction mixture by syringe, upon which the precipitation of $Ru(Me)(I)(CO)_2$-(^{i}Pr-DAB) (3a) started within a few minutes. The mixture was refluxed for another 45 min, cooled to room temperature, and filtered over Celite. The residue was washed with hexane several times to remove excess ^{i}Pr-DAB, and the air-stable product was extracted from the filter with CH_2Cl_2. Evaporation of the solvent yielded complex 3a in about 70% yield (465 mg).[23]

(9) (a) Polm, L. H.; van Koten, G.; Elsevier, C. J.; Vrieze, K.; van Santen, B. F. K.; Stam, C. H. *J. Organomet. Chem.* **1986**, *304*, 353. (b) Muller, F.; Vrieze, K. In *Coordination Chemistry and Catalysis*; Ziolkowski, J. J., Ed.; World Scientific: Singapore, 1988. (c) Elsevier, C. J.; Muller, F.; Vrieze, K.; Zoet, R. *New J. Chem.* **1988**, *12*, 571.

(10) Keijsper, J.; Polm, L. H.; van Koten, G.; Vrieze, K.; Nielsen, E.; Stam, C. H. *Organometallics* **1985**, *4*, 2006.

(11) Staal, L. H.; Polm, L. H.; Balk, R. W.; van Koten, G.; Vrieze, K.; Brouwers, A. M. F. W. *Inorg. Chem.* **1980**, *19*, 3343.

(12) Polm, L. H.; Andrea, R. R.; Elsevier, C. J.; Ernsting, J.-M.; van Koten, G.; Stam, C. H.; Stufkens, D. J.; Vrieze, K. *Organometallics* **1987**, *6*, 1096.

(13) Zoet, R.; Duineveld, C. A.; Elsevier, C. J.; Goubitz, K.; Heijdenrijk, D.; van Koten, G.; Stam, C. H.; Versloot, P.; Vrieze, K.; van Wijnkoop, M. *Organometallics* **1989**, *8*, 23.

(14) Keijsper, J.; Abbel, G.; van Koten, G.; Polm, L. H.; Stam, C. H.; Vrieze, K. *Inorg. Chem.* **1984**, *23*, 2142.

(15) Kraakman, M. J. A.; Elsevier, C. J.; Spek, A. L.; Vrieze, K. *Organometallics*, in press.

(16) $Fe_2(CO)_9$ was prepared by a slightly modified literature procedure by using a quartz Schlenk tube and starting with 25 mL of $Fe(CO)_5$, 150 mL of glacial acetic acid, and 10 mL of acetic anhydride (the last compound was added to prevent the mixture from containing too much water). A Rayonet RS photochemical reactor (λ_{max} = 2500 Å) was used for irradiation, and a continuous stream of air was used to cool the reaction mixture. Filtering, washing subsequently with water, ethanol, and pentane, and drying in vacuo gave $Fe_2(CO)_9$ in usually more than 90% yield. Braye, E. H.; Hübel, W. *Inorg. Synth.* **1966**, *8*, 178.

(17) Roe, D. C. *J. Magn. Reson.* **1985**, *63*, 388.

(18) As described in the Experimental Section, a large excess of MeI is used, which is added in one portion. Since dropwise addition of MeI gives a substantial amount of conversion of 1 to $Ru_2(CO)_6$(^{i}Pr-DAB),[11,14] using the carbonyl ligand liberated by the partial conversion of 1 to 2a, we have to make sure that the reaction with MeI is favored over the reaction with CO, which is achieved by adding a large excess of MeI.

(19) The precipitate formed upon addition of MeI was found to be $[Me_4N][I]$, as was concluded after isolation of the precipitate and a comparison of its ^{1}H NMR spectrum (3.00 ppm in D_2O) with that of commercially obtained $[Me_4N][I]$. During the preparation of 1 by treatment of $Ru_2(CO)_6$(^{i}Pr-DAB) with Me_3NO both CO_2 and NMe_3 are formed as side products. Although the reaction of MeI with NMe_3 to form $[Me_4N][I]$ consumes some MeI, this causes no great problems since a large excess of MeI is used and since $[Me_4N][I]$ can easily be separated from the desired product 2a. (a) Shi, Y.-L.; Gao, Y.-C.; Shi, Q. Z.; Kershner, D. L.; Basolo, F. *Organometalics* **1987**, *6*, 1528. (b) Gao, Y.-C.; Shi, Q. Z.; Kershner, D. L.; Basolo, F. *Inorg. Chem.* **1988**, *27*, 188. (c) Shen, J.-K.; Shi, Y.-L.; Gao, Y.-C.; Shi, Q. Z.; Basolo, F. *J. Am. Chem. Soc.* **1988**, *110*, 2414.

(20) (a) Desrosiers, M. F.; Wink, D. A.; Trautman, R.; Friedman, A. E.; Ford, P. C. *J. Am. Chem. Soc.* **1986**, *108*, 1917. (b) Johnson, B. F. G.; Lewis, J.; Twigg, M. V. *J. Organomet. Chem.* **1974**, *67*, C75.

(21) Mul, W. P.; Elsevier, C. J.; Frühauf, H.-W.; Pein, I.; Stam, C. H.; Vrieze, K.; Zoutberg, M. C. *Inorg. Chem.* **1990**, *29*, 2336.

(22) An excess of α-diimine ligand has to be used to form $Ru(CO)_3$-(α-diimine) in order to prevent the formation of $Ru_2(CO)_6$(α-diimine).[21]

(b) Preparation of Ru(Me)(I)(CO)$_2$(^{i}Pr-Pyca) (3b). A 320-mg amount of $Ru_3(CO)_{12}$ (0.05 mmol) and 400 mg of ^{i}Pr-Pyca (2.7 mmol)[22] were mixed in 50 mL of hexane, 3 mL of MeI was added, and the mixture was refluxed for 1 h. The mixture became dark red within 5 min, and within 10 min the product started precipitating. After 1 h the reaction mixture was cooled to room temperature and filtered over Celite and the residue was washed with hexane several times. The residue was then extracted from the filter with CH_2Cl_2 and the collected extracts were concentrated to 3 mL and purified by column chromatography. Elution with ligroin/CH_2Cl_2 (2/3) afforded a yellow fraction which after evaporation of the solvent yielded Ru(I)$_2$(CO)$_2$(^{i}Pr-Pyca) (**3d**) in 5–10% yield. Elution with CH_2Cl_2 gave rise to a red fraction containing Ru(Me)(I)(CO)$_2$(^{i}Pr-Pyca) (**3b**) in 65–70% yield (450 mg).

(c) i. Preparation of Ru(I)$_2$(CO)$_2$(^{i}Pr-DAB) (3c) from Ru(CO)$_3$(^{i}Pr-DAB) and I$_2$. A 320-mg amount of $Ru_3(CO)_{12}$ (0.5 mmol) and 420 mg of ^{i}Pr-DAB (3 mmol) were refluxed in hexane (60 mL) for 30 min, during which the mixture changed to dark red, indicating that the air-sensitive Ru(CO)$_3$(^{i}Pr-DAB) had been formed.[21,22] The mixture was then cooled to room temperature, after which 400 mg of I_2 (1.56 mmol) in 10 mL of CH_2Cl_2 was added by syringe. Upon addition of the iodine an orange/brown precipitate was formed immediately. The mixture was evaporated to dryness, dissolved in 5 mL of CH_2Cl_2, and purified by column chromatography. The product Ru(I)$_2$(CO)$_2$(^{i}Pr-DAB) (**3c**) was obtained in 60–65% yield (510 mg) as an orange fraction by elution with ligroin/CH_2Cl_2 (2/3). Upon elution with CH_2Cl_2 an orange/brown fraction was obtained containing $Ru_2(I)_4(CO)_6$.[24,25]

ii. Preparation of Ru(I)$_2$(CO)$_2$(^{i}Pr-DAB) (3c) from Ru$_2$(CO)$_6$(^{i}Pr-DAB) and I$_2$. A 255-mg amount of $Ru_2(CO)_6$(^{i}Pr-DAB)[11,14] (0.5 mmol) was dissolved in 30 mL of CH_2Cl_2, and 260 mg of solid I_2 (1.01 mmol) was added, upon which the solution changed from orange to red/brown. The reaction mixture was concentrated to 5 mL and purified by column chromatography as described above. Ru(I)$_2$(CO)$_2$(^{i}Pr-DAB) (**3c**) was isolated in about 80% yield (220 mg).

(d) i. Preparation of Ru(I)$_2$(CO)$_2$(^{i}Pr-Pyca) (3d) from Ru(CO)$_3$(^{i}Pr-Pyca) and I$_2$. A 100-mg amount of $Ru_3(CO)_{12}$ (0.156 mmol) and 150 mg of ^{i}Pr-Pyca (1.01 mmol) were refluxed in 30 mL of hexane, during which the mixture became extremely dark red, indicating that the air-sensitive Ru(CO)$_3$(^{i}Pr-Pyca) had been formed.[22] After 15 min the mixture was cooled to room temperature and 200 mg of I_2 (0.78 mmol) in 10 mL of CH_2Cl_2 was added by syringe, leading to an instantaneous formation of an orange/brown precipitate. The mixture was then evaporated to dryness, dissolved in 5 mL of CH_2Cl_2, and purified by column chromatography. Elution with ligroin/CH_2Cl_2 (2/3) afforded an orange fraction containing Ru(I)$_2$(CO)$_2$(^{i}Pr-Pyca) (**3d**) in about 70% yield (185 mg). Elution with CH_2Cl_2 afforded an orange/brown fraction which contained a small amount of $Ru_2(I)_4(CO)_6$.[24,25]

ii. Preparation of Ru(I)$_2$(CO)$_2$(^{i}Pr-Pyca) (3d) from Ru$_2$(CO)$_4$(^{i}Pr-Pyca)$_2$ and I$_2$. A 305-mg amount of $Ru_2(CO)_4$(^{i}Pr-Pyca)$_2$[12] (0.5 mmol) was dissolved in 40 mL of CH_2Cl_2, and 260 mg of solid I_2 (1.02 mmol) was added. IR spectroscopy indicated the conversion to Ru(I)$_2$(CO)$_2$(^{i}Pr-Pyca) (**3d**) to be instantaneous and quantitative. The mixture was evaporated to dryness and washed with hexane several times to remove excess I_2, and the product usually was used without further purification. This route yielded **3d** in quantitative yields (more than 550 mg in all cases).

(e) Preparation of Ru(benzyl)(Cl)(CO)$_2$(^{i}Pr-DAB) (3e). A 320-mg amount of $Ru_3(CO)_{12}$ (0.5 mmol), 330 mg of ^{i}Pr-DAB (2.36 mmol),[22] and 550 mg of benzyl chloride (4.35 mmol) were refluxed in 60 mL of hexane for 30 min. The reaction mixture was cooled to room temperature, and the precipitate was filtered off. After the precipitate was washed several times with hexane, it was dissolved in 5 mL of CH_2Cl_2 and purified by column chromatography. Elution with CH_2Cl_2 afforded a yellow fraction which contained a small amount of $Ru_2(CO)_5$(IAE).[2,11,14] An orange/red fraction was obtained by elution with acetonitrile, and after evaporation of the solvent Ru(benzyl)(Cl)(CO)$_2$(^{i}Pr-DAB) (**3e**) was isolated in 55–60% yield (360 mg).

5. Preparation of Ru$_2$(Me)(I)(CO)$_4$(PR$_3$)(^{i}Pr-DAB) (PR$_3$ = PPh$_3$ (4a), PMe$_2$Ph (4b), P(OMe)$_3$ (4c)). A 300-mg amount of Ru_2(Me)(I)(CO)$_4$(^{i}Pr-DAB) (**2a**; 0.5 mmol) was dissolved in 50 mL of hexane/CH_2Cl_2 (9/1), and 1 equiv of the phosphine (PR$_3$ = PPh$_3$ (**a**), PMe$_2$Ph (**b**), P(OMe)$_3$ (**c**)) was added. The reaction mixture changed from orange via green to pale yellow, and IR spectroscopy indicated that the reaction proceeded almost instantaneously. The mixture was now concentrated by evaporation of the solvent until precipitation of the product started. Subsequently a small amount of CH_2Cl_2 was added, after which the bright yellow solution was placed at −20 °C overnight, during which a yellow microcrystalline precipitate was formed. After the solvent was removed and the residue dried in vacuo, Ru_2(Me)(I)(CO)$_4$(PR$_3$)(^{i}Pr-DAB) (PR$_3$ = PPh$_3$ (**4a**), PMe$_2$Ph (**4b**), P(OMe)$_3$ (**4c**)) was obtained in about 45% yield. After further concentration of the solution subsequent crystallization led to a total yield of more than 80% in all cases.

6. Reversible Interconversion between 4a–c and 5a–c. (a) Conversion of 4a–c to 5a–c. A solution of 0.5 mmol of Ru_2(Me)(I)(CO)$_4$(PR$_3$)(^{i}Pr-DAB) (PR$_3$ = PPh$_3$ (**4a**), PMe$_2$Ph (**4b**), P(OMe)$_3$ (**4c**)) in 40 mL of hexane/CH_2Cl_2 (19/1) was refluxed until IR spectroscopy indicated that the conversion to Ru_2(Me)(I)(CO)$_3$(PR$_3$)(^{i}Pr-DAB) (PR$_3$ = PPh$_3$ (**5a**), PMe$_2$Ph (**5b**), P(OMe)$_3$ (**5c**)) was complete (2–3 h). **5a–c** were isolated by crystallization from the reaction mixture at −20 °C in yields of up to 80% (in solution the conversion is quantitative).

(b) Conversion of 5a–c to 4a–c. A solution of 0.5 mmol of **5a–c** was stirred under an atmosphere of carbon monoxide at room temperature. The solution rapidly changed from yellow to dark green and then gradually back to yellow. IR spectroscopy only showed the absorptions belonging to the complexes **5a–c** and **4a–c**, whereas no absorptions belonging to the green intermediate were observed. After about 10 min IR spectroscopy indicated that the conversion to **4a–c** was complete and **4a–c** were isolated as described above (vide supra).

7. Reaction of Ru(Me)(I)(CO)$_2$(^{i}Pr-DAB) (3a) with Ru$_3$(CO)$_{12}$ To Give Ru$_2$(Me)(I)(CO)$_4$(^{i}Pr-DAB) (2a) and Ru$_2$(C(O)Me)(I)(CO)$_4$(^{i}Pr-DAB) (8). A 440-mg amount of Ru(Me)(I)(CO)$_2$(^{i}Pr-DAB) (**3a**; 1 mmol) and 240 mg of $Ru_3(CO)_{12}$ (0.38 mmol) were dissolved in 60 mL of toluene and refluxed until IR spectroscopy indicated that the reaction was complete (about 90 min). The solvent was evaporated at a temperature of 50 °C; the residue was dissolved in 5 mL of CH_2Cl_2 and purified by column chromatography. Elution with ligroin/CH_2Cl_2 (9/1) gave a yellow fraction containing the unreacted $Ru_3(CO)_{12}$, whereas elution with ligroin/CH_2Cl_2 (7/3) afforded an orange fraction which contained Ru_2(Me)(I)(CO)$_4$(^{i}Pr-DAB) (**2a**) in about 65% yield (385 mg). Subsequently a yellow fraction was eluted with ligroin/CH_2Cl_2 (4/6) which after evaporation of the solvent afforded Ru_2(C(O)Me)(I)(CO)$_4$(^{i}Pr-DAB) (**8**) in 15% yield (90 mg).[26]

8. Reaction of Ru(Me)(I)(CO)$_2$(^{i}Pr-DAB) (3a) with Fe$_2$(CO)$_9$ To Give FeRu(CO)$_4$(^{i}Pr-DAB) (2b) and HFeRu(Me)(CO)$_5$(^{i}Pr-DAB) (6). A 220-mg amount of Ru(Me)(I)(CO)$_2$(^{i}Pr-DAB) (**3a**; 0.5 mmol) was dissolved in 25 mL of a solvent (hexane, diethyl ether, benzene, CH_2Cl_2, or THF) and the mixture stirred in the presence of an excess of $Fe_2(CO)_9$ until IR spectroscopy indicated that the absorptions belonging to **3a** were no longer present. Depending on the solvent, 3 (hexane) to 6 (THF) equiv of $Fe_2(CO)_9$ was used. The unreacted $Fe_2(CO)_9$ was filtered

(23) It should be noted for the preparation of **3a** that IR spectroscopy indicated in some cases the presence of small amounts of $Ru_3(CO)_{12}$. Purification by column chromatography was then applied.

(24) Johnson, B. F. G.; Johnston, R. D.; Lewis, J. *J. Chem. Soc. A* **1969**, 792.

(25) The ruthenium halide clusters formed during the reaction were usually identified as $Ru_3(I)_6(CO)_{12}$ or as a mixture of $Ru_3(I)_6(CO)_{12}$ and $Ru_2(I)_4(CO)_6$. However, after purification in all cases only $Ru_2(I)_4(CO)_6$ could be isolated. This observation agrees with literature data, since it has been reported already that $Ru_3(I)_6(CO)_{12}$ easily converts to $Ru_2(I)_4(CO)_6$. For more information see: Bruce, M. I. In *Comprehensive Organometallic Chemistry*; Wilkinson, G., Stone, F. G. A., Abel, E. W., Eds.; Pergamon Press: Oxford, U.K., 1982; Vol. IV, Chapter 32, p 673.

(26) The formation of the acetyl complex **8** as a side product in the reaction of **3a** and Ru(CO)$_4$ may be explained by a reaction of **3a** with CO to produce Ru(C(O)Me)(I)(CO)$_2$(^{i}Pr-DAB) before reaction with a Ru(CO)$_4$ fragment takes place. A separate experiment showed that in refluxing heptane **3a** slowly reacts with CO to give Ru(C(O)Me)(I)(CO)$_2$(^{i}Pr-DAB).

Table I. Crystallographic Data for $Ru_2(Me)(I)(CO)_4(^iPr\text{-}DAB)$ (2a), $Ru_2(CO)_4(Me)(I)(PMe_2Ph)(^iPr\text{-}DAB)$ (4b), and $HFeRu(Me)(CO)_5(^iPr\text{-}DAB)$ (6)

	2a	4b	6
		Crystal Data	
formula	$C_{13}H_{19}IN_2O_4Ru_2$	$C_{21}H_{30}IN_2O_4PRu_2$	$C_{14}H_{20}FeN_2O_5Ru$
mol wt	596.35	734.50	453.24
cryst syst	orthorhombic	monoclinic	monoclinic
space group	*Pbca* (No. 61)	$P2_1/c$ (No. 14)	$C2/c$ (No. 15)
a, Å	16.2510 (10)	7.2030 (10)	18.102 (4)
b, Å	13.2660 (10)	21.907 (2)	8.2761 (6)
c, Å	17.2410 (10)	16.813 (3)	25.131 (4)
β, deg		94.352 (13)	90.627 (16)
V, Å^3	3716.9 (4)	2645.4 (6)	3764.6 (11)
D_{calc}, g cm^{-3}	2.131	1.844	1.599
Z	8	4	8
F(000)	2272	1432	1824
μ, cm^{-1}	32.6	23.6	15.8
cryst size, mm	0.10 × 0.33 × 0.45	0.20 × 0.22 × 0.68	0.18 × 0.26 × 0.58
		Data Collection	
temp, K	295	295	295
radiation	Mo Kα (Zr filter), 0.71073 Å	Mo Kα (Zr filter), 0.71073 Å	Mo Kα (Zr filter), 0.71073 Å
$\theta_{min}/\theta_{max}$, deg	1.2/29.4	1.0/27.5	1.0/27.5
Δω, deg	0.60 + 0.35 tan θ	1.0 + 0.35 tan θ	0.99 + 0.35 tan θ
horiz/vert aperture, mm	3.00/6.00	3.00/6.00	3.36/5.00
X-ray exposure time, h	79.3	112.5	105.7
linear decay, %			17
ref reflns	021; 430; 302	21$\bar{1}$; 22$\bar{2}$; 162	206; 425; 532
data set	0–22; 0–18; 0–23	0–9; 0–28; −21 to +21	−23 to +23; −10 to 0; −32 to +32
total no. of data	5740	7583	7456
no. of unique data	4758	6074	4307
R_{int}	0.065	0.035	0.054
no. of obsd data	3387 ($I > 2.5\sigma(I)$)	4118 ($I > 2.5\sigma(I)$)	2740 ($I > 2.5\sigma(I)$)
abs cor range	1.24, 1.93 (ABSORB)	0.84, 1.10 (DIFABS)	1.31, 1.53 (ABSORB)
		Refinement	
no. of refined params	216	300	228
no. of rflns	3382	4118	2740
R, R_w, S	0.031, 0.039, 2.21	0.047, 0.059, 3.01	0.042, 0.041, 2.79
weighting scheme	$1/\sigma^2(F)$	$1/\sigma^2(F)$	$1/\sigma^2(F)$
U overall isotropic H atoms	0.080 (5), 0.046 (6)	0.077 (7), 0.071 (9)	0.121 (7), 0.073 (7)
$(\Delta/\sigma)_{av}$ in final cycle	0.05	0.022	0.016
max/min residual density, e Å^{-3}	−0.70/+0.68	−1.68/+0.98	−0.53/+0.82

off, and the $Fe(CO)_5$[27] formed was removed by evaporating the reaction mixture to dryness. The residue was dissolved in 3 mL of CH_2Cl_2 and purified by column chromatography. Elution with ligroin afforded a green fraction which contained $Fe_3(CO)_{12}$.[27] Elution with ligroin/CH_2Cl_2 (3/2) gave a red fraction which after evaporation of the solvent yielded $FeRu(CO)_4(^iPr\text{-}DAB)$ (**2b**) in 65–70% yield (185 mg).

It should be noted that the use of extremely dry solvents is very important in this reaction, since traces of water led to the formation of $HFeRu(Me)(CO)_5(^iPr\text{-}DAB)$ (**6**) (vide infra).

9. Synthesis of $HFeRu(Me)(CO)_5(^iPr\text{-}DAB)$ (6). A 220-mg amount of $Ru(Me)(I)(CO)_2(^iPr\text{-}DAB)$ (**3a**; 0.5 mmol) was dissolved in 25 mL of a solvent (hexane, benzene), and 100 μL of H_2O was added. The mixture was then stirred in the presence of $Fe_2(CO)_9$ for 3 h (benzene) or 16 h (hexane), after which the excess $Fe_2(CO)_9$ was filtered off. The reaction mixture was then evaporated to dryness and purified by column chromatography. Elution with ligroin afforded a green fraction which contained $HFeRu(Me)(CO)_5(^iPr\text{-}DAB)$ (**6**) and $Fe_3(CO)_{12}$. Elution with ligroin/CH_2Cl_2 (3/2) yielded a red fraction containing $FeRu(Me)(I)(CO)_4(^iPr\text{-}DAB)$ (**2b**) in about 60% yield (165 mg).

The green fraction was concentrated to 10 mL and allowed to stand at −60 °C overnight. The precipitated $Fe_3(CO)_{12}$ was then filtered off, and the resulting solution contained $HFeRu(Me)(CO)_5(^iPr\text{-}DAB)$ (**6**) in about 20% yield (45 mg).

10. Synthesis of $Ru_2(I)_2(CO)_4(^iPr\text{-}DAB)$ (7) from $Ru(I)_2(CO)_2(^iPr\text{-}DAB)$ (3c). A 300-mg amount of $Ru(I)_2(CO)_2(^iPr\text{-}DAB)$ (**3c**; 0.54 mmol) and 220 mg of $Ru_3(CO)_{12}$ (0.31 mmol) were suspended in 50 mL of hexane and refluxed for 5 h, during which the reaction mixture turned into a clear red solution. The reaction mixture was cooled to room temperature and brought upon a column for purification. Elution with ligroin/CH_2Cl_2 (9/1) gave a yellow fraction containing the unreacted $Ru_3(CO)_{12}$. An orange fraction containing a small amount of unidentified product was obtained by elution with ligroin/CH_2Cl_2 (4/1). Finally, elution with ligroin/CH_2Cl_2 (1/1) afforded a red fraction which contained $Ru_2(I)_2(CO)_4(^iPr\text{-}DAB)$ (**7**) in about 70% yield (265 mg).

11. High-Pressure NMR Experiments. A 50-mg amount of $Ru_2(Me)(I)(CO)_4(^iPr\text{-}DAB)$ (**2a**) was dissolved in 1.5 mL of the appropriate solvent (C_6D_6 or $CDCl_3$) and syringed into the sapphire tube, which was kept under an atmosphere of dinitrogen using a specially designed glass vessel. The tube was then connected to a high-pressure system, if necessary placed in a bath of acetone and solid CO_2, and pressurized over 15 min. The NMR tube was then closed and disconnected from the high-pressure system, and the reaction was monitored by means of NMR spectroscopy.

12. X-ray Structure Determination of $Ru_2(Me)(I)(CO)_4(^iPr\text{-}DAB)$ (2a), $Ru_2(Me)(I)(CO)_4(PMe_2Ph)(^iPr\text{-}DAB)$ (4b), and $HFeRu(Me)(CO)_5(^iPr\text{-}DAB)$ (6). Crystal data and numerical details of the structure determinations are given in Table I. Crystals suitable for X-ray structure determination were mounted on a Lindemann glass capillary and transferred to an Enraf-Nonius CAD-4F diffractometer for data collection. Lattice parameters were determined by least-squares fitting of the SET4 setting angles of 25 reflections with 14.1° < θ < 18.1°, 12.5° <

(27) $Fe(CO)_5$ and $Fe(CO)_4$ are formed from $Fe_2(CO)_9$. The $Fe(CO)_4$ fragments that do not react with complex 1 trimerize, forming $Fe_3(CO)_{12}$. See also: (a) Shriver, D. F.; Whitmire, K. H. In *Comprehensive Organometallic Chemistry*; Wilkinson, G., Stone, F. G. A., Abel, E. W., Eds.; Pergamon Press: Oxford, U.K., 1982; Vol. IV, pp 255–258. (b) King, R. B. *Organometallic Synthesis*; Academic Press: New York, London, 1965; Vol. 1, p 94. (c) King, R. B.; Stone, F. G. A. *Inorg. Synth.* **1965**, *7*, 193. (d) Fehlhammer, W. P.; Herrmann, W. A.; Öfele, K. In *Handbuch der Präparativen Anorganischen Chemie* 3rd ed.; Ferdinand Enke Verlag: Stuttgart, 1981; pp 1827–1829.

Scheme I. Observed Reaction Sequence for the Formation of Complexes 3a, 4a–c, and 5a–c

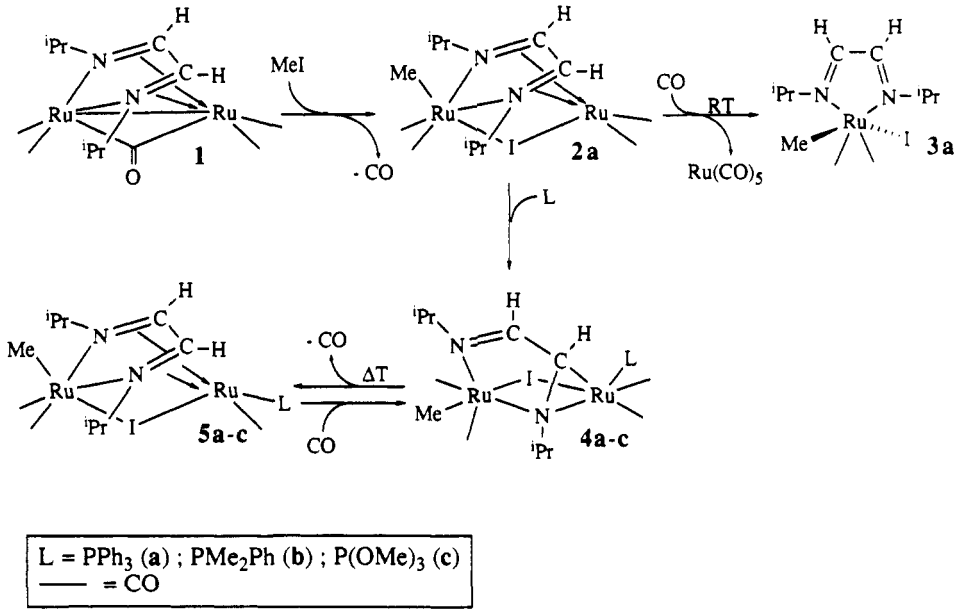

$\theta < 17.9°$, and $10.7° < \theta < 16.2°$ for **2a**, **4b**, and **6**, respectively. The unit-cell parameters were checked for the presence of higher lattice symmetry.[28] Data were collected with the $\omega/2\theta$ scan mode. All data were corrected for Lp and for the observed linear decay of the reference reflections. Absorption correction was applied for **2a** and **6** using ABSORB (Gaussian integration) and for **4b** using the DIFABS procedure.[29] Standard deviations of the intensities as obtained by counting statistics were increased according to an analysis of the excess variance of the reference reflections: $\sigma^2(I) = \sigma_{cs}^2(I) + (pI)^2$, with $p = 0.049$, 0.026, and 0.027 for **2a**, **4b**, and **6**, respectively.[30] The structures were solved by automated standard Patterson methods followed by tangent expansion (**2a**, **4b**) or automated direct methods (**6**).[31] Refinement on F was carried out by full-matrix least-squares techniques.[32] The hydrogen atoms were included in the refinement on calculated positions (C–H = 0.98 Å) riding on their carrier atoms. The hydride hydrogen atom of **6** was located on a difference Fourier map; its coordinates were included in the refinement. All non-hydrogen atoms were refined with anisotropic thermal parameters; the hydrogen atoms of **2a**, **4b**, and **6** were refined with two common isotropic thermal parameters, one for the methyl group and the phenyl group of **4b** and one for the other hydrogen atoms. Weights were introduced in the final refinement cycles. Atomic scattering factors were taken from Cromer and Mann;[33] anomalous-dispersion corrections were obtained from Cromer and Liberman.[34] Geometric calculations and illustrations were performed with PLATON[35] on a MicroVAX cluster and a DEC station 5000.

Results and Discussion

Preparation of the Complexes 2a,b, 3a–e, 4a–c, 5a–c, and 6–8. The dinuclear complex $Ru_2(Me)(I)(CO)_4(^iPr\text{-}DAB)$ **(2a)** has been obtained from $Ru_2(CO)_5(^iPr\text{-}DAB)$ **(1)** and MeI in good yields. Reaction of **2a** with carbon monoxide and PR_3 led to the formation of the complexes $Ru(Me)(I)(CO)_2(^iPr\text{-}DAB)$ **(3a)**, $Ru_2(Me)(I)(CO)_4(PR_3)(^iPr\text{-}DAB)$ **(4a–c)**, and $Ru_2(Me)(I)(CO)_3(PR_3)(^iPr\text{-}DAB)$ **(5a–c)** according to the sequence outlined in Scheme I. The mononuclear complexes $Ru(X)(Y)(CO)_2(\alpha\text{-diimine})$ **(3a–e)** have also been obtained via several other routes that have been summarized in Scheme II. Finally, the reactions of the mononuclear complexes **3a** and **3c** with unsaturated fragments $M(CO)_4$ (prepared from $Ru_3(CO)_{12}$ (M = Ru) or $Fe_2(CO)_9$ (M = Fe)) resulted in the formation of

Table II. Fractional Coordinates and Equivalent Isotropic Thermal Parameters for the Non-Hydrogen Atoms of $Ru_2(Me)(I)(CO)_4(^iPr\text{-}DAB)$ (2a) (with Esd's in Parentheses)

	x	y	z	U_{eq},[a] Å^2
I	0.12416 (2)	0.17497 (2)	0.26827 (2)	0.0516 (1)
Ru1	0.07372 (2)	0.37295 (2)	0.27079 (2)	0.0369 (1)
Ru2	0.04512 (2)	0.24655 (3)	0.41703 (3)	0.0334 (1)
O1	−0.0207 (3)	0.3954 (3)	0.1216 (2)	0.0770 (16)
O2	0.2166 (3)	0.4826 (3)	0.1965 (3)	0.0760 (14)
O3	−0.0659 (2)	0.0700 (3)	0.4456 (2)	0.0623 (14)
O4	0.1630 (3)	0.1406 (3)	0.5224 (3)	0.0913 (19)
N1	−0.0335 (2)	0.3330 (3)	0.34196 (19)	0.0325 (10)
N2	0.1090 (2)	0.3862 (3)	0.3934 (2)	0.0387 (11)
C1	0.0173 (3)	0.3844 (4)	0.1767 (3)	0.0510 (17)
C2	0.1639 (3)	0.4395 (4)	0.2241 (3)	0.0520 (17)
C3	−0.0227 (3)	0.1355 (3)	0.4328 (3)	0.0417 (14)
C4	0.1197 (3)	0.1812 (4)	0.4812 (3)	0.0513 (17)
C5	−0.0106 (3)	0.3162 (4)	0.5141 (3)	0.0483 (17)
C6	−0.1144 (2)	0.3026 (4)	0.3077 (3)	0.0430 (16)
C7	−0.1077 (3)	0.2074 (4)	0.2604 (3)	0.0507 (16)
C8	−0.1775 (3)	0.2918 (4)	0.3730 (3)	0.0540 (16)
C9	−0.0205 (3)	0.4355 (3)	0.3451 (2)	0.0397 (12)
C10	0.0582 (3)	0.4641 (3)	0.3736 (3)	0.0413 (16)
C11	0.1918 (3)	0.4196 (4)	0.4216 (3)	0.0537 (17)
C12	0.2586 (3)	0.3446 (5)	0.3989 (4)	0.074 (3)
C13	0.1898 (4)	0.4365 (5)	0.5084 (3)	0.071 (2)

[a] $U_{eq} = {}^1/_3\sum_i\sum_j U_{ij}a_i^*a_j^*\mathbf{a}_i\mathbf{a}_j$.

Table III. Bond Distances (Å) for the Non-Hydrogen Atoms of $Ru_2(Me)(I)(CO)_4(^iPr\text{-}DAB)$ (2a) (with Esd's in Parentheses)

Ru1–Ru2	3.0635 (6)	I–Ru1	2.7517 (5)	I–Ru2	3.0215 (5)
Ru1–N1	2.196 (3)	Ru1–N2	2.197 (3)	Ru1–C1	1.870 (5)
Ru1–C2	1.891 (5)	Ru1–C9	2.162 (4)	Ru1–C10	2.160 (5)
Ru2–N1	2.150 (4)	Ru2–N2	2.162 (4)	Ru2–C3	1.860 (4)
Ru2–C4	1.856 (5)	Ru2–C5	2.115 (5)	O1–C1	1.142 (6)
O2–C2	1.134 (7)	O3–C3	1.139 (6)	O4–C4	1.136 (7)
N1–C6	1.497 (5)	N1–C9	1.377 (6)	N2–C10	1.366 (6)
N2–C11	1.498 (6)	C6–C7	1.507 (7)	C6–C8	1.530 (7)
C9–C10	1.422 (7)	C11–C12	1.524 (8)	C11–C13	1.514 (7)

(28) Spek, A. L. *J. Appl. Crystallogr.* **1988**, *21*, 578.
(29) Walker, N.; Stuart, D. *Acta Crystallogr., Sect. A* **1983**, *A39*, 158.
(30) McCandlish, L. E.; Stout, G. H.; Andrews, L. C. *Acta Crystallogr., Sect. A* **1975**, *31*, 245.
(31) Sheldrick, G. M. *SHELXS86*, Program for crystal structure determination; University of Göttingen, Göttingen, Germany, 1986.
(32) Sheldrick, G. M. *SHELX76*, Program for crystal structure determination; University of Cambridge, Cambridge, England, 1976.
(33) Cromer, D. T.; Mann, J. B. *Acta Crystallogr., Sect. A* **1968**, *24*, 321.
(34) Cromer, D. T.; Liberman, D. *J. Chem. Phys.* **1970**, *53*, 1891.
(35) Spek, A. L. *Acta Crystallogr., Sect. A* **1990**, *46*, C34.

Scheme II. Synthetic Routes for the Preparation of Ru(R)(X)(CO)$_2$(N-N) (3a–e)

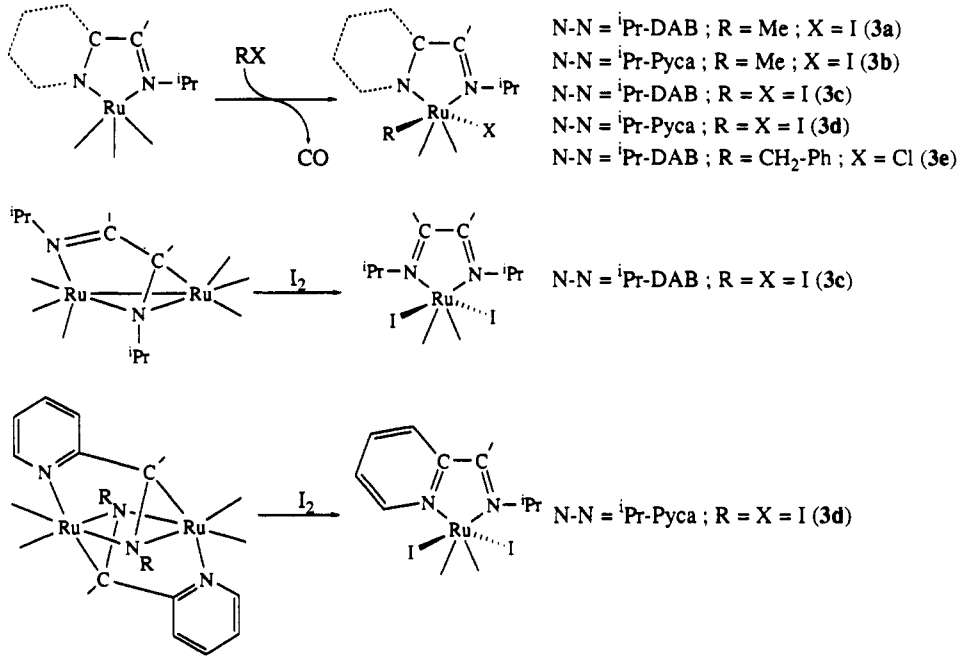

Scheme III. Reactions of Complexes 3 with M(CO)$_4$ Fragments, Yielding 2a,b and 6–8

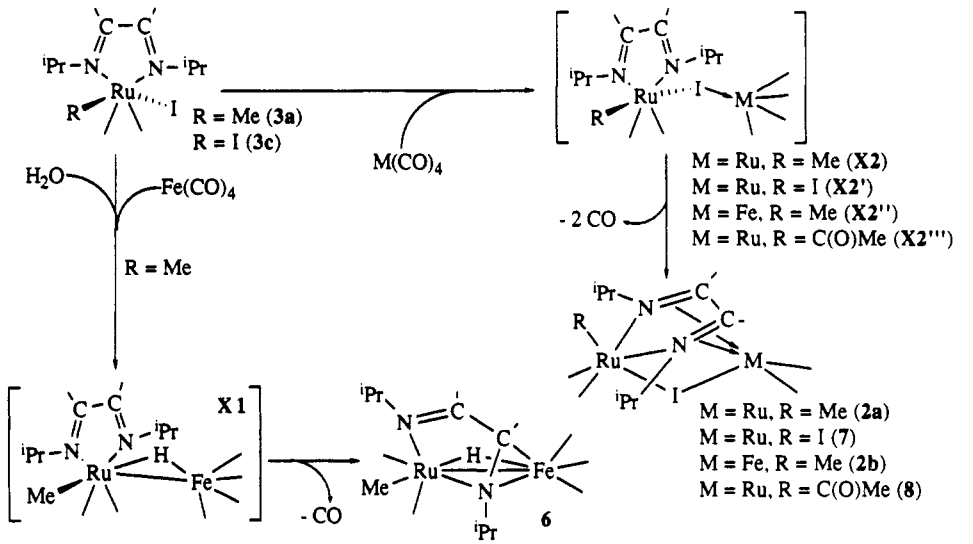

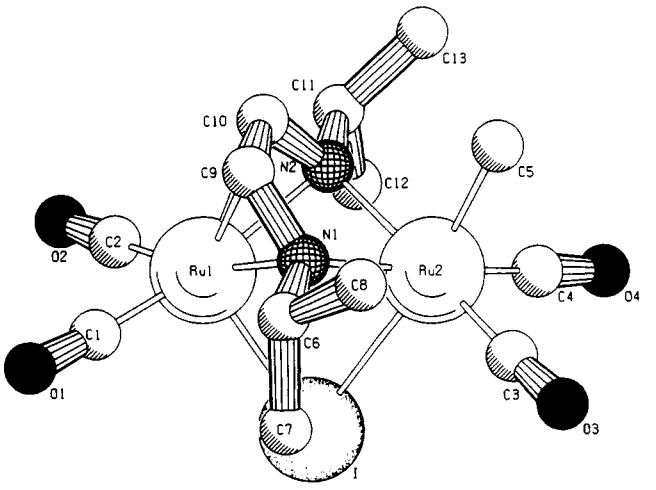

Figure 2. Molecular structure of Ru$_2$(Me)(I)(CO)$_4$(^{i}Pr-DAB) (**2a**).

2a and the new complexes FeRu(Me)(I)(CO)$_4$(^{i}Pr-DAB) (2b), HFeRu(Me)(CO)$_5$(^{i}Pr-DAB) (6), Ru$_2$(I)$_2$(CO)$_4$(^{i}Pr-DAB) (7), and small amounts of the side product Ru$_2$(C(O)Me)(I)(CO)$_4$(^{i}Pr-DAB) (8) (Scheme III). In the following we will first discuss the structural and spectroscopic aspects of the relevant complexes and subsequently deal with the aspects of their formation.

Molecular Structure of Complex 2a. The molecular structure of **2a** is shown in Figure 2 together with the atomic numbering, the fractional coordinates of the non-hydrogen atoms of **2a** are listed in Table II. Table III contains the bond lengths of the non-hydrogen atoms of complex **2a**, whereas in Table IV the bond angles of the non-hydrogen atoms are listed.

The molecular structure consists of a Ru(Me)(CO)$_2$ fragment and a Ru(CO)$_2$ fragment, held together by an iodide bridge and a bridging α-diimine ligand. The distance between the two metal atoms is rather long (3.0635 (6) Å), since Ru–Ru bonds usually vary from 2.70 to 2.90 Å,[10,14,21,36–39] and in the case of **2a** the Ru–Ru distance is

(36) Bennet, M. A.; Bruce, M. I.; Matheson, T. W. In *Comprehensive Organometallic Chemistry*; Wilkinson, G., Stone, F. G. A., Abel, E. W., Eds.; Pergamon Press: Oxford, U.K., 1982; Chapter 32.4, pp 821–841.

Table IV. Bond Angles (deg) for the Non-Hydrogen Atoms of $Ru_2(Me)(I)(CO)_4(^iPr\text{-}DAB)$ (2a) (with Esd's in Parentheses)

Ru1-I-Ru2	63.90 (1)	Ru1-N1-C9	70.2 (2)	C2-Ru1-C10	100.3 (2)
I-Ru1-N1	90.85 (10)	Ru2-N1-C9	114.3 (3)	I-Ru2-Ru1	53.77 (1)
I-Ru1-C1	102.12 (16)	Ru1-N2-Ru2	89.28 (14)	I-Ru2-N2	84.56 (9)
I-Ru1-C9	125.92 (11)	Ru1-N2-C11	124.8 (3)	I-Ru2-C4	94.68 (16)
Ru2-Ru1-N1	44.57 (9)	Ru2-N2-C11	128.6 (3)	Ru1-Ru2-N1	45.79 (9)
Ru2-Ru1-C1	133.17 (16)	Ru1-C1-O1	175.6 (5)	Ru1-Ru2-C3	130.08 (16)
Ru2-Ru1-C9	67.35 (10)	Ru2-C3-O3	176.5 (4)	Ru1-Ru2-C5	118.49 (14)
N1-Ru1-N2	71.87 (12)	N1-C6-C7	112.1 (3)	N1-Ru2-C3	99.11 (18)
N1-Ru1-C2	164.91 (19)	C7-C6-C8	111.6 (4)	N1-Ru2-C5	89.36 (17)
N1-Ru1-C10	65.42 (16)	Ru1-C9-C10	70.7 (3)	N2-Ru2-C4	101.48 (18)
N2-Ru1-C2	99.79 (18)	Ru1-C10-C9	70.9 (3)	C3-Ru2-C4	86.0 (2)
N2-Ru1-C10	36.52 (16)	C9-C10-N2	115.4 (4)	C4-Ru2-C5	90.7 (2)
C1-Ru1-C9	97.80 (19)	N2-C11-C13	110.2 (4)	Ru1-N1-C6	122.8 (3)
C2-Ru1-C9	128.46 (19)	I-Ru1-Ru2	62.34 (1)	Ru2-N1-C6	128.0 (3)
C9-Ru1-C10	38.40 (17)	I-Ru1-N2	90.79 (10)	C6-N1-C9	114.6 (4)
I-Ru2-N1	84.79 (9)	I-Ru1-C2	102.01 (16)	Ru1-N2-C10	70.3 (3)
I-Ru2-C3	97.30 (15)	I-Ru1-C10	125.59 (12)	Ru2-N2-C10	113.90 (13)
I-Ru2-C5	172.23 (14)	Ru2-Ru1-N2	44.89 (10)	C10-N2-C11	113.6 (4)
Ru1-Ru2-N2	45.82 (9)	Ru2-Ru1-C2	136.35 (16)	Ru1-C2-O2	177.6 (5)
Ru1-Ru2-C4	130.33 (16)	Ru2-Ru1-C10	67.26 (12)	Ru2-C4-O4	177.4 (5)
N1-Ru2-N2	73.43 (13)	N1-Ru1-C1	96.62 (17)	N1-C6-C8	108.9 (4)
N1-Ru2-C4	174.91 (19)	N1-Ru1-C9	36.83 (15)	Ru1-C9-N1	72.9 (2)
N2-Ru2-C3	172.18 (17)	N2-Ru1-C1	162.98 (18)	N1-C9-C10	114.5 (4)
N2-Ru2-C5	88.87 (17)	N2-Ru1-C9	65.42 (14)	Ru1-C10-N2	73.2 (2)
C3-Ru2-C5	88.7 (2)	C1-Ru1-C2	88.4 (2)	N2-C11-C12	111.3 (4)
Ru1-N1-Ru2	89.63 (12)	C1-Ru1-C10	127.5 (2)	C12-C11-C13	111.5 (5)

close to the nonbonding distance of 3.1012 (6) Å in $Ru_3(CO)_8(\mu\text{-}CH_2)(^n\text{Pent-DAB})$.[40] The long Ru–Ru distance therefore indicates that no effective metal–metal bond is present in **2a**, which is in agreement with the 18-electron rule.

A striking aspect of the structure is the difference in the bond lengths of Ru1–I (2.7517 (5) Å) and Ru2–I (3.0215 (5) Å). This is very likely due to trans effects, since a methyl group is known to be a strong trans-labilizing ligand.[41]

The ^{i}Pr-DAB ligand is coordinated to Ru2 via both nitrogen atoms with approximately equal distances (2.150 (4) and 2.162 (4) Å), comparable to those reported for $Ru_2(CO)_5(^i\text{Pr-DAB})$,[14] which are indicative for a chelate coordination with respect to Ru2. The ^{i}Pr-DAB ligand is coordinated to Ru1 via N1, C9, C10, and N2 with comparable Ru1–N and Ru1–C bond lengths (Ru1–N1 = 2.196 (3) Å, Ru1–C9 = 2.162 (4) Å, Ru1–C10 = 2.160 (5) Å, Ru1–N2 = 2.197 (3) Å). The observed virtually equal values of the Ru1–N and Ru1–C bond lengths are in agreement with values reported for other complexes that contain a DAB ligand in the 8e $\sigma(N)\text{-}\sigma(N')\text{-}\eta^2(C{=}N)\text{:}\eta^2(C{=}N')$ coordination mode, as for example $Ru_2(CO)_4(HC{\equiv}CH)(DAB)$,[42] $Ru_2(CO)_5(DAB)$,[14] and $Ru_4(CO)_8(DAB)_2$.[39]

The C=N bond lengths within the α-diimine ligand are relatively short in **2a** (1.372 (4) Å (mean)) compared to values reported for $Ru_2(CO)_4(HC{\equiv}CH)(DAB)$ (1.423 Å (mean)[42]), $Ru_2(CO)_5(DAB)$ (1.43 Å (mean)[14]), and $Ru_4(CO)_8(DAB)_2$ (1.41 Å (mean)[39]), whereas the central C–C bond of **2a** is rather long (1.422 (7) Å for **2a** vs 1.369 (11),[42] 1.39 (2),[14] and 1.41 Å (mean),[39] respectively). Since the LUMO of a DAB ligand is antibonding between the two C=N bonds and bonding between the central C atoms, the observed bond lengths indicate that there is limited π back-bonding from Ru1 to the DAB ligand, suggesting a relatively weak $\eta^2(C{=}N)$-metal bonding for **2a**. This agrees with the observation that the imine–metal bonding can easily be substituted.

The molecule contains a noncrystallographic mirror plane through the methyl group, the two metal atoms, and the iodide bridge. The ^{i}Pr-DAB ligand is coordinated perfectly symmetrically, as can be seen from the equal distances to the mirror plane of C9 and C10 (0.710 (8) and 0.712 (8) Å, respectively), N1 and N2 (1.289 (7) and 1.289 (8) Å, respectively) and even C6 and C11 (2.784 (7) and 2.786 (9) Å, respectively). This agrees with the angle between the C(9)–C(10) bond and the mirror plane, which is almost perpendicular (89.6 (3)°).

The four carbonyl ligands are not perfectly symmetrically coordinated, as can be seen from their distances to the mirror plane (1.308 (9) vs 1.224 (9) Å for C3 and C4, respectively, and 1.341 (7) vs 1.280 (7) Å for C1 and C2, respectively).

Finally, it is noteworthy to mention the unusually large angle of 24.7 (2)° between the plane formed by N1Ru2N2 and the plane formed by N1C9C10N2 compared to values of 6.5, 10, and 14° that were reported for $Ru_2(CO)_5(DAB)$,[14] $Mn_2(CO)_6(MeN{=}C(Me)\text{-}C(Me){=}NMe)$,[43] and $Ru_2(CO)_4(HC{\equiv}CH)(DAB)$,[42] respectively.

Molecular Structure of Complex 4b. The molecular structure of **4b** is shown in Figure 3 together with the atomic numbering; Tables V–VII contain the fractional coordinates, the bond lengths, and the bond angles of the non-hydrogen atoms of **4b**, respectively.

The molecular structure of **4b** consists of a $Ru(Me)(CO)_2$ fragment and a $Ru(CO)_2(PMe_2Ph)$ fragment which are bridged by an iodide atom and a 6e-donating $\sigma(N)\text{-}\mu_2(N')\text{-}\eta^2(C{=}N)$-bonded DAB ligand. As far as we know, only one crystal structure determination has been reported before in the literature of a 6e $\sigma(N)\text{-}\mu_2(N')\text{-}\eta^2(C{=}N')$-coordinated DAB ligand with an $\eta^2(C{=}N)$ unit bonded to Ru.[11]

(37) Bruce, M. I. In *Comprehensive Organometallic Chemistry*; Wilkinson, G., Stone, F. G. A., Abel, E. W., Eds.; Pergamon Press: Oxford, U.K., 1982; Vol. IV, Chapter 32.5, p 846.
(38) Keijsper, J.; van Koten, G.; Polm, L. H.; Seignette, P. F. A. B.; Stam, C. H.; Vrieze, K. *Inorg. Chem.* **1985**, *24*, 518.
(39) Staal, L. H.; Polm, L. H.; Ploeger, F.; Stam, C. H.; Vrieze, K. *Inorg. Chem.* **1981**, *20*, 3590.
(40) Keijsper, J.; Goubitz, K.; van Koten, G.; Polm, L. H.; Stam, C. H.; Vrieze, K. *Organometallics* **1985**, *4*, 1876.
(41) (a) Huheey, J. E. In *Inorganic Chemistry*, 3rd ed.; Harper Collins: New York, 1983; pp 538–545. (b) Zumdahl, S. S.; Drago, R. S. *J. Am. Chem. Soc.* **1968**, *90*, 6669.
(42) Staal, L. H.; van Koten, G.; Ploeger, F.; Stam, C. H.; Vrieze, K. *Inorg. Chem.* **1981**, *20*, 1830.
(43) Adams, R. D. *J. Am. Chem. Soc.* **1980**, *102*, 7476.

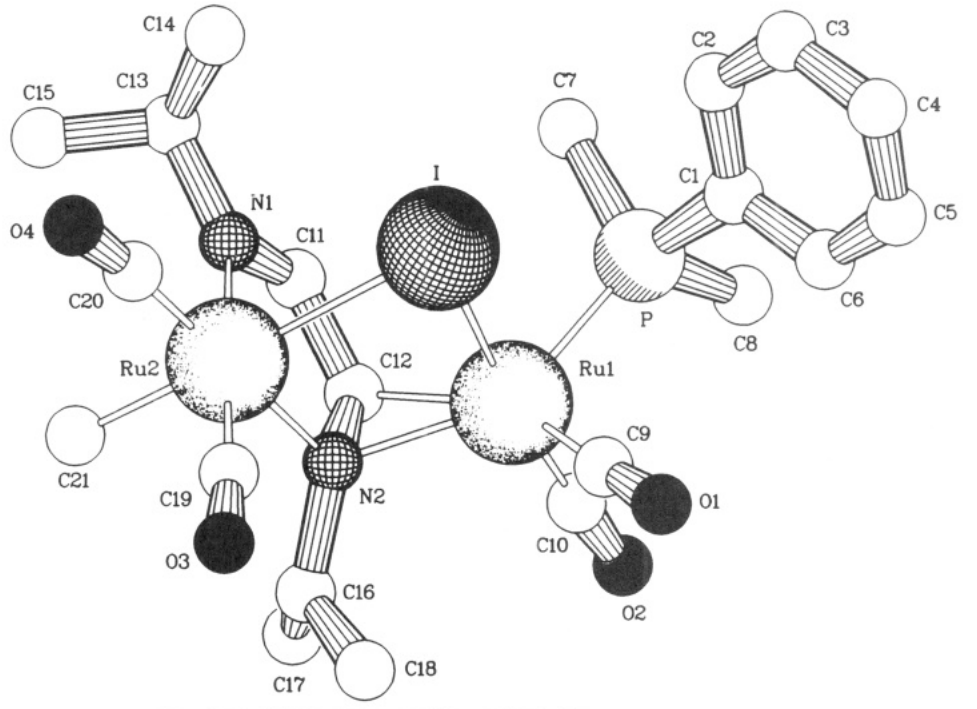

Figure 3. Molecular structure of $Ru_2(Me)(I)(CO)_4(PMe_2Ph)(^iPr\text{-}DAB)$ (**4b**).

Table V. Fractional Coordinates and Equivalent Isotropic Thermal Parameters of the Non-Hydrogen Atoms of $Ru_2(Me)(I)(CO)_4(PMe_2Ph)(^iPr\text{-}DAB)$ (4b) (with Esd's in Parentheses)

	x	y	z	U_{eq},[a] Å^2
I	0.96002 (8)	0.07292 (3)	0.14361 (3)	0.0520 (2)
Ru1	1.14678 (8)	0.15227 (3)	0.25094 (3)	0.0324 (2)
Ru2	1.10402 (8)	−0.00934 (3)	0.26077 (4)	0.0376 (2)
P	1.2284 (3)	0.21022 (10)	0.14147 (12)	0.0410 (7)
O1	0.7563 (9)	0.2043 (3)	0.2640 (4)	0.071 (3)
O2	1.3132 (9)	0.2513 (3)	0.3567 (4)	0.069 (3)
O3	0.7696 (10)	−0.0221 (4)	0.3538 (4)	0.092 (3)
O4	0.9645 (12)	−0.1245 (4)	0.1819 (6)	0.104 (4)
N1	1.3534 (8)	0.0024 (3)	0.2023 (4)	0.040 (2)
N2	1.2162 (8)	0.0723 (3)	0.3222 (3)	0.0367 (19)
C1	1.0324 (11)	0.2313 (3)	0.0709 (4)	0.039 (2)
C2	1.0023 (14)	0.2032 (4)	−0.0028 (5)	0.057 (3)
C3	0.8538 (17)	0.2201 (5)	−0.0529 (6)	0.074 (4)
C4	0.7337 (12)	0.2647 (4)	−0.0312 (5)	0.054 (3)
C5	0.7670 (11)	0.2928 (4)	0.0400 (5)	0.048 (3)
C6	0.9114 (11)	0.2759 (4)	0.0911 (5)	0.042 (3)
C7	1.3914 (14)	0.1723 (5)	0.0815 (6)	0.069 (4)
C8	1.3409 (14)	0.2824 (4)	0.1624 (6)	0.064 (4)
C9	0.8996 (11)	0.1837 (4)	0.2594 (4)	0.043 (3)
C10	1.2522 (11)	0.2116 (4)	0.3168 (5)	0.049 (3)
C11	1.4391 (10)	0.0521 (4)	0.2249 (5)	0.042 (3)
C12	1.3723 (10)	0.0911 (3)	0.2864 (4)	0.039 (3)
C13	1.4386 (12)	−0.0354 (5)	0.1405 (5)	0.060 (3)
C14	1.3109 (15)	−0.0371 (6)	0.0644 (6)	0.080 (4)
C15	1.4884 (15)	−0.0979 (4)	0.1716 (7)	0.073 (4)
C16	1.2177 (14)	0.0755 (5)	0.4126 (5)	0.070 (4)
C17	1.3810 (19)	0.0914 (7)	0.4559 (6)	0.115 (7)
C18	1.0433 (15)	0.0987 (6)	0.4404 (6)	0.076 (4)
C19	0.8970 (11)	−0.0154 (4)	0.3176 (5)	0.051 (3)
C20	1.0240 (14)	−0.0800 (5)	0.2086 (6)	0.064 (4)
C21	1.2581 (14)	−0.0642 (4)	0.3454 (6)	0.059 (3)

[a] $U_{eq} = {}^1/_3\sum_i\sum_j U_{ij}a_i^*a_j^*\mathbf{a}_i\mathbf{a}_j$.

The Ru–Ru distance in **4b** is 3.5587 (11) Å, which, in agreement with the 18e rule, clearly indicates the absence of a metal–metal bond. As in complex **2a**, the iodide is coordinated trans toward the methyl group (C21–Ru2–I = 169.9 (3)°). However, in **4b** the Ru2–I distance is substantially shorter than in **2a** (2.8095 (10) Å in **4b** vs 3.0215 (5) Å in **2a**). This shortening of the Ru2–I bond might indicate that the best description of the bonding situation

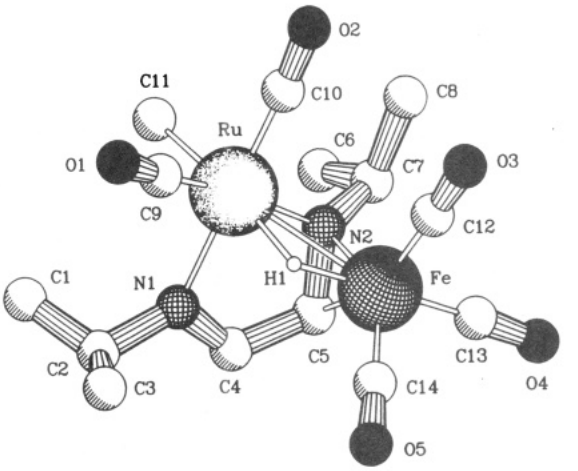

Figure 4. Molecular structure of $HFeRu(Me)(CO)_5(^iPr\text{-}DAB)$ (**6**).

in **4b** is that the iodide is σ-bonded to Ru2 and has a 2e-donor bond to Ru1. The fact that the Ru2–I distance is still rather long for a σ-bonded iodide may be rationalized by the trans-labilizing effect of the methyl group. In this context one may compare the Ru–I bond lengths of **4b** with those found for the *trans*-I_2 complex $Ru(I)_2(CO)_2(^pTol\text{-}DAB)$, for which a Ru–I distance of 2.708 (1) Å has been reported.[44]

The N2–C12 bond length of 1.378 (9) Å is significantly elongated as compared to the C=N double-bond length in free ^{c}Hex-DAB (1.258 (3) Å),[45] which is a consequence of electron donation from the metal into the antibonding π* orbitals of the DAB ligand.[1,11,46]

Interesting features of the structure are the Ru2–CO bond lengths. The coordination of carbonyl ligand C10O2

(44) tom Dieck, H.; Kollvitz, W.; Kleinwächter, I.; Rohde, W.; Stamp, L. *Transition Met. Chem.* **1986**, *11*, 361.
(45) Keijsper, J.; van Koten, G.; van der Poel, H.; Polm, L. H.; Seignette, P. F. A. B.; Varenhorst, R.; Stam, C. H.; Vrieze, K. *Polyhedron* **1983**, *2*, 1111.
(46) Zoet, R.; Goubitz, K.; van Halen, C. J. G.; van Koten, G.; Vrieze, K. *Inorg. Chim. Acta* **1988**, *149* (2), 193.

Table VI. Bond Distances (Å) for the Non-Hydrogen Atoms of $Ru_2(Me)(I)(CO)_4(PMe_2PH)(^iPr\text{-}DAB)$ (4b) (with Esd's in Parentheses)

I-Ru1	2.7784 (10)	I-Ru2	2.8095 (10)	Ru1-P	2.347 (2)
Ru1-N2	2.160 (6)	Ru1-C9	1.924 (8)	Ru1-C10	1.834 (9)
Ru1-C12	2.155 (7)	Ru2-N1	2.128 (6)	Ru2-N2	2.189 (6)
Ru2-C19	1.836 (8)	Ru2-C20	1.850 (11)	Ru2-C21	2.112 (10)
P-C1	1.833 (8)	P-C7	1.807 (11)	P-C8	1.799 (9)
O1-C9	1.135 (10)	O2-C10	1.164 (11)	O3-C19	1.148 (11)
O4-C20	1.143 (14)	N1-C11	1.294 (11)	N1-C13	1.496 (11)
N2-C12	1.378 (9)	N2-C16	1.521 (10)	C1-C2	1.386 (11)
C1-C6	1.369 (11)	C2-C3	1.362 (15)	C3-C4	1.373 (14)
C4-C5	1.351 (12)	C5-C5	1.350 (12)	C11-C12	1.451 (11)
C13-C14	1.519 (13)	C13-C15	1.499 (14)	C16-C17	1.380 (16)
C16-C18	1.464 (15)				

Table VII. Bond Angles (deg) for the Non-Hydrogen Atoms of $Ru_2(Me)(I)(CO)_4(PMe_2Ph)(^iPr\text{-}DAB)$ (4b) (with Esd's in Parentheses)

Ru1-I-Ru2	79.11 (3)	P-C1-C2	121.8 (6)	N2-Ru2-C19	95.7 (3)
I-Ru1-N2	86.16 (15)	C2-C1-C6	118.6 (7)	N2-Ru2-C21	89.5 (3)
I-Ru1-C10	173.4 (3)	C2-C3-C4	120.7 (9)	C19-Ru2-C21	90.8 (4)
P-Ru1-N2	144.35 (16)	C4-C5-C6	121.0 (8)	Ru1-P-C1	114.7 (3)
P-Ru1-C10	88.5 (3)	Ru1-C9-O1	177.5 (8)	Ru1-P-C8	117.2 (3)
N2-Ru1-C9	115.2 (3)	N1-C11-C12	121.9 (7)	C1-P-C8	102.6 (4)
N2-Ru1-C12	37.3 (2)	Ru1-C12-C11	116.9 (5)	Ru2-N1-C11	111.5 (5)
C9-Ru1-C12	152.2 (3)	N1-C13-C14	110.2 (8)	C11-N1-C13	117.2 (7)
I-Ru2-N1	83.01 (18)	C14-C13-C15	112.6 (9)	Ru1-N2-C12	71.2 (4)
I-Ru2-C19	98.1 (3)	N2-C16-C18	113.2 (8)	Ru2-N2-C12	108.8 (4)
I-Ru2-C21	169.9 (3)	Ru2-C19-O3	176.7 (8)	C12-N2-C16	118.6 (6)
N1-Ru2-C19	175.4 (3)	I-Ru1-P	88.10 (6)	P-C1-C6	119.5 (6)
N1-Ru2-C21	87.8 (3)	I-Ru1-C9	82.3 (2)	C1-C2-C3	119.6 (9)
N2-Ru2-C20	176.5 (4)	I-Ru1-C12	96.22 (18)	C3-C4-C5	119.1 (8)
C19-Ru2-C20	87.1 (4)	P-Ru1-C9	98.8 (2)	C1-C6-C5	120.8 (8)
C20-Ru2-C21	88.4 (4)	P-Ru1-C12	108.96 (19)	Ru1-C10-O2	176.6 (7)
Ru1-P-C7	113.6 (4)	N2-Ru1-C10	99.9 (3)	Ru1-C12-N2	71.6 (4)
C1-P-C7	104.8 (4)	C9-Ru1-C10	92.6 (3)	N2-C12-C11	117.4 (6)
C7-P-C8	102.2 (5)	C10-Ru1-C12	90.3 (3)	N1-C13-C15	111.3 (7)
Ru2-N1-C13	131.2 (5)	I-Ru2-N2	84.85 (15)	N2-C16-C17	118.7 (8)
Ru1-N2-Ru2	109.8 (2)	I-Ru2-C20	96.8 (3)	C17-C16-C18	117.5 (9)
Ru1-N2-C16	120.1 (5)	N1-Ru2-N2	79.9 (2)	Ru2-C20-O4	173.8 (10)
Ru2-N2-C16	118.9 (5)	N1-Ru2-C20	97.2 (4)		

Table VIII. Fractional Coordinates and Equivalent Isotropic Thermal Parameters for the Non-Hydrogen Atoms of $HFeRu(Me)(CO)_5(^iPr\text{-}DAB)$ (6) (with Esd's in Parentheses)

	x	y	z	U_{eq},[a] Å^2
Ru	0.26890 (2)	0.16608 (5)	0.35647 (2)	0.0481 (1)
Fe	0.33109 (4)	0.02288 (10)	0.44722 (3)	0.0625 (3)
O1	0.1527 (2)	0.4224 (6)	0.3548 (2)	0.103 (2)
O2	0.3711 (3)	0.4492 (5)	0.3499 (2)	0.0936 (18)
O3	0.4065 (3)	0.3242 (7)	0.4771 (2)	0.120 (3)
O4	0.4450 (3)	−0.1719 (8)	0.4982 (3)	0.155 (3)
O5	0.2284 (3)	−0.0359 (7)	0.5335 (2)	0.117 (3)
N1	0.1964 (2)	−0.0387 (5)	0.35919 (16)	0.0550 (16)
N2	0.3467 (2)	−0.0191 (5)	0.37078 (17)	0.0527 (14)
C1	0.0901 (4)	−0.0016 (11)	0.3000 (3)	0.109 (4)
C2	0.1150 (3)	−0.0550 (8)	0.3524 (2)	0.074 (2)
C3	0.0769 (3)	0.0177 (11)	0.3982 (3)	0.103 (3)
C4	0.2308 (3)	−0.1605 (7)	0.3785 (2)	0.0597 (17)
C5	0.3092 (3)	−0.1500 (6)	0.3913 (2)	0.0593 (19)
C6	0.4134 (4)	−0.1448 (9)	0.2981 (3)	0.095 (3)
C7	0.4211 (3)	−0.0574 (7)	0.3502 (3)	0.069 (2)
C8	0.4690 (3)	0.0926 (8)	0.3458 (4)	0.107 (3)
C9	0.1955 (3)	0.3198 (7)	0.3550 (3)	0.069 (2)
C10	0.3342 (3)	0.3382 (7)	0.3529 (2)	0.0647 (19)
C11	0.2695 (3)	0.1543 (8)	0.2716 (2)	0.075 (2)
C12	0.3770 (4)	0.2060 (9)	0.4662 (3)	0.088 (3)
C13	0.4022 (4)	−0.0951 (9)	0.4766 (3)	0.098 (3)
C14	0.2691 (4)	−0.0128 (8)	0.4997 (3)	0.081 (3)

[a] $U_{eq} = {}^1/_3\sum_i\sum_j U_{ij}a_i^*a_j^*\mathbf{a}_i\mathbf{a}_j$.

Table IX. Bond Distances (Å) for the Non-Hydrogen Atoms of $HFeRu(Me)(CO)_5(^iPr\text{-}DAB)$ (6) (with Esd's in Parentheses)

Ru-Fe	2.7959 (11)	Ru-N1	2.145 (4)	Ru-N2	2.110 (4)
Ru-C9	1.840 (6)	Ru-C10	1.854 (6)	Ru-C11	2.135 (5)
Fe-N2	1.976 (4)	Fe-C5	2.041 (5)	Fe-C12	1.791 (7)
Fe-C13	1.771 (7)	Fe-C14	1.766 (7)	O1-C9	1.149 (7)
O2-C10	1.139 (7)	O3-C12	1.146 (9)	O4-C13	1.136 (10)
O5-C14	1.147 (9)	N1-C2	1.488 (7)	N1-C4	1.278 (7)
N2-C5	1.381 (7)	N2-C7	1.482 (7)	C1-C2	1.456 (9)
C2-C3	1.476 (9)	C4-C5	1.454 (8)	C6-C7	1.501 (10)
C7-C8	1.519 (8)				

is normal as is that of the carbonyls with Ru2. However, the C9–O1 bond length (1.135 (10) Å) is rather short and at the same time the Ru1–C9 bond length (1.924 (8) Å) is very long, indicating that this ligand is relatively weakly coordinated to Ru1, as appears to be corroborated by the observed easy elimination of CO from **4b**.

Molecular Structure of Complex 6. The molecular structure of **6** is shown in Figure 4 together with the atomic numbering; Tables VIII–X contain the fractional coordinates, the bond lengths, and the bond angles of the non-hydrogen atoms of **6**, respectively.

As shown in Figure 4, the molcule contains an Fe–Ru bond with a bond length of 2.7959 (11) Å. This is not an extremely large value for an Fe–Ru bond, which usually varies from 2.60 to 2.80 Å with the average being approximately 2.69 Å.[47] This value, however, represents a rather long distance as compared to, for instance, the value of 2.6602 (9) Å reported for $FeRu(CO)_6(^iPr\text{-}DAB)$[46] or 2.653 (3) Å for $FeRu(CO)_6(^iPr\text{-}Pyca)$.[48] This relatively long

(47) (a) Venäläinen, T.; Pakkanen, T. *J. Organomet. Chem.* **1984**, *266*, 269. (b) Roberts, D. A.; Geoffroy, G. L. In *Comprehensive Organometallic Chemistry*; Wilkinson, G., Stone, F. G. A., Abel, E. W., Eds.; Pergamon Press: Oxford, U.K., 1982; Chapter 40.

(48) Kraakman, M. J. A.; Elsevier, C. J.; Ernsting, J.-M.; Goubitz, K.; Vrieze, K. *Inorg. Chim. Acta*, in press.

Table X. Bond Angles (deg) for the Non-Hydrogen Atoms of HFeRu(Me)(CO)$_5$(^{i}Pr-DAB) (6) (with Esd's in Parentheses)

N1-Ru-N2	80.10 (15)	N1-C2-C3	110.1 (4)	C12-Fe-C13	91.3 (3)
N1-Ru-C10	177.8 (2)	N1-C4-C5	120.5 (5)	C13-Fe-C14	93.5 (3)
N2-Ru-C9	170.6 (3)	Fe-C5-C4	112.1 (4)	Ru-N1-C4	109.9 (3)
N2-Ru-C11	97.3 (2)	N2-C7-C6	109.4 (5)	Ru-N2-Fe	86.31 (16)
C9-Ru-C11	91.3 (3)	C6-C7-C8	112.2 (6)	Ru-N2-C7	134.7 (4)
N2-Fe-C5	40.19 (19)	Ru-C10-O2	176.2 (5)	Fe-N2-C7	121.1 (4)
N2-Fe-C13	101.4 (3)	Fe-C13-O4	175.6 (7)	N1-C2-C1	111.9 (5)
C5-Fe-C12	149.6 (3)	N1-Ru-C9	96.0 (2)	C1-C2-C3	116.0 (6)
C5-Fe-C14	106.1 (3)	N1-Ru-C11	90.3 (2)	Fe-C5-N2	67.3 (3)
C12-Fe-C14	103.9 (3)	N2-Ru-C10	98.1 (2)	N2-C5-C4	116.5 (4)
Ru-N1-C2	132.2 (4)	C9-Ru-C10	85.9 (2)	N2-C7-C8	111.9 (5)
C2-N1-C4	116.7 (5)	C10-Ru-C11	88.7 (2)	Ru-C9-O1	176.0 (5)
Ru-N2-C5	107.7 (3)	N2-Fe-C12	109.7 (3)	Fe-C12-O3	178.4 (7)
Fe-N2-C5	72.5 (3)	N2-Fe-C14	142.7 (3)	Fe-C14-O5	179.5 (7)
C5-N2-C7	114.5 (4)	C5-Fe-C13	92.0 (3)		

Table XI. IR Data and Elemental Analyses for the Complexes 2a,b, 3a–e, 4a–c, 5a–c, and 6–8

complex	IR ν(C≡O), cm^{-1}	obsd (calcd) elemental anal., % C	H	N
2a[a]	2040 (m), 2022 (vs), 1976 (s), 1959 (s)	26.20 (26.18)	3.25 (3.21)	4.76 (4.70)
2b[a]	2030 (m), 2012 (vs), 1969 (s), 1956 (s)	28.28 (28.33)	3.36 (3.47)	5.06 (5.08)
3a[c]	2031 (s), 1966 (s)	30.04 (30.08)	4.23 (4.36)	5.81 (6.38)
3b[c]	2030 (s), 1962 (s)	31.18 (32.23)	3.44 (3.38)	6.11 (6.26)
3c[c]	2057 (s), 2002 (s)	21.71 (21.79)	2.86 (2.93)	5.12 (5.08)
3d[c]	2053 (s), 1997 (s)	23.75 (23.63)	2.22 (2.16)	5.12 (5.01)
3e[c]	2032 (s), 1967 (s)	48.09 (48.17)	5.45 (5.47)	6.73 (6.61)
4a[a]	2020 (s), 2005 (s), 1945 (vs, br)	43.27 (43.36)	4.06 (3.99)	3.22 (3.26)
4b[a]	2019 (s), 2002 (s), 1942 (sh), 1937 (vs, br)	34.28 (34.34)	4.16 (4.12)	3.86 (3.81)
4c[a]	2029 (s), 2015 (s), 1960 (sh), 1948 (vs, br)	26.49 (26.67)	3.98 (3.92)	3.84 (3.88)
5a[a]	2019 (s), 1947 (vs, br)	42.76 (43.38)	4.18 (4.13)	3.52 (3.37)
5b[a]	2019 (s), 1944 (vs, br)		not analyzed[d]	
5c[a]	2018 (s), 1955 (sh), 1945 (vs, br)	26.13 (26.02)	4.07 (4.08)	3.97 (4.05)
6[b]	2055 (s), 2018 (vs), 1985 (vs), 1980 (vs), 1958 (s)		not analyzed[e]	
7[b]	2055 (m), 2034 (vs), 1995 (vs), 1979 (s)	20.46 (20.35)	2.35 (2.28)	3.89 (3.96)
8[a]	2039 (w), 2026 (vs), 1974 (s, br), 1967 (sh), 1675 (vw)	27.01 (26.93)	3.05 (3.07)	4.56 (4.49)

[a] In hexane/CH_2Cl_2 (9/1). [b] In hexane. [c] In CH_2Cl_2. [d] Not analyzed since no solvent-free sample was obtained. [e] Not analyzed since yields of solvent-free crystalline material were very low.

metal–metal bond can be rationalized by the presence of the bridging hydride, since hydride ligands generally have a lengthening effect on metal–metal bonds.[37]

The 6e-donating DAB ligand is coordinated to ruthenium via both nitrogen atoms with similar bond lengths (2.145 (4) and 2.110 (4) Å for Ru–N1 and Ru–N2, respectively). These values are analogous to those reported for FeRu(CO)$_6$(^{i}Pr-DAB) (2.138 (4) and 2.102 (3) Å). The DAB ligand is coordinated to iron via an η^2(C=N) linkage and, as for **4b**, the bond length of the η^2-bonded C=N moiety is strongly elongated (1.381 (7) Å) compared to a value of 1.258 (3) Å for an uncoordinated DAB ligand.[45]

It is clear that the elongation of the coordinated imine bond is substantially less in complex **6** as compared to the elongation observed for FeRu(CO)$_6$(^{i}Pr-DAB) (1.414 (6) Å).[46] This might be rationalized by describing the Fe center of **6** as Fe(I) due to the presence of the hydride ligand. In comparison to the iron in FeRu(CO)$_6$(^{i}Pr-DAB), the iron center of **6** is more electron deficient, which results in donation of less electron density to the π* orbitals of the coordinated imine bond.

A final point to be mentioned is the torsion angle N1–C5–C4–N2, which in complex **6** is −14.2 (7)°, indicating a relatively large distortion from planarity of the metallacycle as compared to the case in complex **4b**, in which the torsion angle N1–C11–C12–N2 amounts to only 2.1 (11)°. However, the heterometallic core might be the reason for this large torsion angle, which has also been observed for the heteronuclear complexes FeRu(CO)$_6$(^{i}Pr-DAB) (13°) and FeRu(CO)$_6$(^{i}Pr-Pyca) (17°).[48]

IR Spectroscopy and Analyses. The IR spectroscopic data are listed in Table XI together with the results of the elemental analyses. The position of the absorptions in all cases indicates the presence of terminal carbonyl ligands. Complexes **3a–e** show two absorption of approximately equal intensity, indicating a cis arrangement of the two carbonyl ligands, since a trans arrangement would give rise to only one absorption or to two absorptions of very different intensities.[49]

NMR Spectroscopy. The NMR spectroscopic data are listed in Tables XII and XIII. As can be seen from the tables, complexes **2a,b** show ^{1}H NMR resonances for the imine protons around 6 ppm, whereas the corresponding carbon signals in the ^{13}C NMR spectrum were observed around 105 ppm. These values agree with a DAB ligand in the 8e σ(N)-σ(N′)-η^2(C=N):η^2(C=N′) coordination mode. Since the X-ray structure of **2a** shows the carbonyl ligands to be asymmetrically coordinated with respect to the mirror plane of the molecule, one would expect four carbonyl signals. However, the ^{13}C NMR spectra show only one signal for the carbonyl ligands coordinated to Ru2 and one signal for the carbonyls coordinated to Ru1 (**2a**) or Fe (**2b**). This probably means that in solution the carbonyls coordinated to the same metal are magnetically equivalent on the NMR time scale.

The NMR data for **3a,c** are in agreement with the reported values.[44,50] In the case of the new complexes **3b,d,e** it may be concluded that the organic group and the halide

(49) (a) Glyde, R. W.; Mawby, R. J. *Inorg. Chim. Acta* **1971**, *5*, 317. (b) Adams, D. M. In *Metal-Ligand and Related Vibrations*; Edward Arnold: London, 1967; p 103. (c) Pankowski, M.; Bigorgne, M. *J. Organomet. Chem.* **1977**, *125*, 231. (d) Pankowski, M.; Bigorgne, M. *J. Organomet. Chem.* **1971**, *30*, 227.

(50) (a) Rohde, W.; tom Dieck, H.; Klaus, J. *J. Organomet. Chem.* **1987**, *328*, 209. (b) tom Dieck, H.; Rohde, W.; Behrens, U. *Z. Naturforsch.* **1989**, *44B*, 158.

Table XII. ^{1}H NMR Data[a] for the Complexes 2a,b, 3a–e, 4a–c, 5a–c, and 6–8 and Intermediates X2 and X3

2a	6.08 (2 H, s, N=CH); 2.73 (2 H, sept, 6.3 Hz, ^{i}Pr CH); 1.66/1.36 (6 H/6 H, d, 6.3 Hz, ^{i}Pr CH_3); 0.35 (3 H, s, Me)
2b	5.92 (2 H, s, N=CH); 2.77 (2 H, sept, 6.5 Hz, ^{i}Pr CH); 1.69/1.37 (6 H/6 H, d, 6.5 Hz, ^{i}Pr CH_3); 0.23 (3 H, s, Ru—Me)
3a[b]	8.17 (2 H, s, N=CH); 4.47 (2 H, sept, 6.5 Hz, ^{i}Pr CH); 1.57/1.53 (6 H/6 H, d, 6.5 Hz, ^{i}Pr CH_3); -0.04 (3 H, s, Ru—Me)
3b	8.91 (1 H, d, 5 Hz, py H6); 8.53 (1 H, s, N=CH); 7.95 (2 H, m, py H3/H4); 7.50 (1 H, dd, 7 Hz/5 Hz, py H5); 4.36 (1 H, sept, 6.5 Hz, ^{i}Pr CH); 1.59/1.51 (3 H/3 H, d, 6.5 Hz, ^{i}Pr CH_3); -0.02 (3 H, s, Ru—Me)
3c[b]	8.17 (2 H, s, N=CH); 4.61 (2 H, sept, 6.6 Hz, ^{i}Pr CH); 1.65 (6 H, d, 6.6 Hz, ^{i}Pr CH_3)
3d	9.04 (1 H, d, 5 Hz, py H6); 8.51 (1 H, s, N=CH); 8.07 (2 H, m, py H3/H4); 7.65 (1 H, dd, 7 Hz/5 Hz, py H5); 4.51 (1 H, sept. 6.5 Hz, ^{i}Pr CH); 1.65 (6 H, d, 6.5 Hz, ^{i}Pr CH_3)
3e	8.12 (2 H, s, N=CH); 7.05 (2 H, dd, 7.1 Hz/7.6 Hz, Ph H3/H5); 6.88 (1 H, dd, 7.1 Hz/7.6 Hz, Ph H4); 6.82 (2 H, d, 7.1 Hz, Ph H2/H6); 4.08 (2 H, sept, 6 Hz, ^{i}Pr CH); 2.19 (2 H, s, Ru—CH_2—Ph); 1.52/1.32 (6 H/6 H, d, 6 Hz, ^{i}Pr CH_3)
4a	7.68–7.36 (16 H, m, P—C_6H_5 + σ-N=CH); 3.96 (1 H, s, η^2-N=CH); 3.66/3.15 (1 H/1 H, sept, 6.5 Hz, ^{i}Pr CH); 1.35/1.24/1.11 (6 H/3 H/3 H, d, 6.5 Hz, ^{i}Pr CH_3); 0.21 (3 H, s, Ru—Me)
4b	7.60–7.35 (6 H, m, P—C_6H_5 + σ-N=CH); 3.78 (1 H, d, 1 Hz, η^2-N=CH); 3.69/3.06 (1 H/1 H, sept, 6.7 Hz, ^{i}Pr CH); 1.89/1.86 (3 H/3 H, d, 9.2 Hz, P—CH_3); 1.29/1.25/1.19/0.90 (3 H/3 H/3 H/3 H, d, 6.7 Hz, ^{i}Pr CH_3); 0.17 (3 H, s, Ru—Me)
4c	8.17 (1 H, s, σ-N=CH); 4.47/3.65 (1 H/1 H, sept, 6.6 Hz, ^{i}Pr CH); 3.64 (9 H, d, 12 Hz, P—OCH_3); 3.58 (1 H, s, η^2-N=CH); 1.31/1.27/1.22/0.86 (3 H/3 H/3 H/3 H, d, 6.6 hz, ^{i}Pr CH_3); 0.14 (3 H, s, Ru—Me)
5a	7.70–7.60/7.40–7.30 (6 H/9 H, m, P—C_6H_5); 5.81/5.78 (1 H/1 H, s, N=CH); 2.81 (1 H, sept, 6.6 Hz, ^{i}Pr CH); 1.97 (1 H, sept, 6.2 Hz, ^{i}Pr CH); 1.82/1.37 (3 H/3 H, 3, 6.6 Hz, ^{i}Pr CH_3); 0.99/0.75 (3 H/3 H, d, 6.2 Hz, ^{i}Pr CH_3); 0.26 (3 H, s, Ru—Me)
5b	7.55–7.38 (5 H, m, P—C_6H_5); 5.70/5.46 (1 H/1 H, s, N=CH); 2.72/2.10 (1 H/1 H, sept, 6.5 Hz, ^{i}Pr CH); 1.94/1.80 (3 H/3 H, d, 9.1 Hz, P—CH_3); 1.73/1.34/1.09 (3 H/6 H/3 H, d, 6.5 Hz, ^{i}Pr CH_3); 0.28 (3 H, s, Ru—Me)
5c	5.89/5.82 (1 H/1 H, s, N=CH); 3.59 (9 H, d, 11.8 Hz, P—CH_3); 2.87/2.74 (1 H/1 H, sept, 6.4 Hz, ^{i}Pr CH); 1.73/1.57/1.35/1.29 (3 H/3 H/3 H/3 H, d, 6.4 Hz, ^{i}Pr CH_3); 0.30 (3 H, s, Ru—Me)
6	7.84 (1 H, s, σ-N=CH); 3.50/2.96 (1 H/1 H, sept, 6.6 Hz, ^{i}Pr CH); 3.40 (1 H, s, η^2-N=CH); 1.64/1.43/1.13/1.10 (3 H/3 H/3 H/3 H, d, 6.6 Hz, ^{i}Pr CH_3); 0.80 (3 H, s, Ru—Me); -16.45 (1 H, s, Ru—H)
7	6.28 (2 H, s, N=CH); 2.79 (2 H, sept, 6.6 Hz, ^{i}Pr CH); 1.74/1.64 (6 H/6 H, d, 6.6 Hz, ^{i}Pr CH_3); 0.06 (3 H, s, Ru—Me)
8	6.17 (2 H, s, N=CH); 2.66 (2 H, sept, 6.4 Hz, ^{i}Pr CH); 2.47 (3 H, s, C(O)CH_3); 1.46/1.13 (6 H/6 H, d, 6.4 hz, ^{i}Pr CH_3)
X2[c]	8.31 (2 H, s, σ-N=CH); 3.12 (2 H, sept (br), ^{i}Pr CH); 0.14 (3 H, s, Ru—Me)
X3[c]	8.85 (1 H, d, 1 Hz, σ-N=CH); 4.24/4.06 (1 H/1 H, sept, 6.5 Hz, ^{i}Pr CH); 4.14 (1 H, d, 1 Hz, η^2-N=CH); 0.23 (3 H, s, Ru—Me)

[a] In $CDCl_3$ solution at 300 MHz and 243 K unless stated otherwise. [b] Observed data in agreement with ref 44 and 50. [c] In $CDCl_3$ solution at 300 MHz and 228 K.

Table XIII. ^{13}C NMR Data[a] for the Complexes 2a,b, 3a–e, 4a–c, 5a–c, and 6–8

2a	-3.0 (Ru—CH_3); 25.2/27.6 (^{i}Pr CH_3); 64.1 (^{i}Pr CH); 104.4 (N=CH); 200.3/198.1 (CO)
2b	-2.3 (Ru—CH_3); 26.0/27.6 (^{i}Pr CH_3); 65.1 (^{i}Pr CH); 105.9 (N=CH); 200.5 (Ru—CO); 207.7 (Fe—CO)
3a	-5.5 (Ru—CH_3); 24.2/24.8 (^{i}Pr CH_3); 66.0 (^{i}Pr CH); 158.1 (N=CH); 202.1 (CO)
3b	-4.8 (Ru—CH_3); 24.2/24.9 (^{i}Pr CH_3); 65.9 (^{i}Pr CH); 127.9 (py C^5); 128.9 (py C^3); 139.0 (py C^4); 152.7 (py C^6); 153.7 (py C^2); 161.0 (N=CH); 202.3/202.9 (CO)
3c	25.2 (^{i}Pr CH_3); 66.7 (^{i}Pr CH); 160.1 (N=CH); 197.5 (CO)
3d	24.5 (^{i}Pr CH_3); 65.9 (^{i}Pr CH); 128.2 (py C^5); 129.2 (py C^3); 139.6 (py C^4); 153.4 (py C^6); 153.6 (py C^2); 162.8 (N=CH); 196.5/197.2 (CO)
3e	14.0 (Ru—CH_2—Ph); 22.7/24.0 (^{i}Pr CH_3); 64.6 (^{i}Pr CH); 123.8 (Ph C^4); 127.4/128.7 (Ph C^2/C^3/C^5/C^6); 151.0 (Ph C^1); 159.1 (N=CH); 200.9 (CO)
4a	-2.5 (Ru—CH_3); 21.7/24.9/28.0/30.6 (^{i}Pr CH_3); 63.1 (br, η^2-N=CH); 64.1/65.7 (^{i}Pr CH); 128.7 (d, 9.9 Hz, Ph C^3/C^5); 130.4 (Ph C^4); 133.4 (d, 11.3 hz, Ph C^2/C^6); 135.5 (d, 42.2 Hz, Ph C^1); 169.2 (σ-N=CH); 197.4 (d, 14.9 Hz, Ru(P)$(CO)_2$); 201.2 (d, 2.4 Hz, Ru(P)$(CO)_2$); 200.6/203.4 (Ru$(CO)_2$)
4b	-2.2 (Ru—(CH_3); 19.1 (d, 31 Hz, P—CH_3); 19.8 (d, 32 Hz, P—CH_3); 25.2/27.9/30.4/31.3 (^{i}Pr CH_3); 62.8 (br, η^2-N=CH); 63.3/63.6 (^{i}Pr CH); 129.1 (d, 9.4 Hz, Ph C^3/C^5); 129.4 (d, 9.8 Hz, Ph C^2/C^6); 130.1 (d, 2.3 Hz, Ph C^4); 141.6 (d, 41.1 Hz, Ph C^1); 168.8 (σ-N=CH); 198.1 (d, 15.4 Hz, Ru(P)$(CO)_2$); 199.9 (d, 3 Hz, Ru(P)$(CO)_2$); 200.8/203.5 (Ru$(CO)_2$)
4c	-2.8 (Ru—CH_3); 21.3/24.6/28.1/30.6 (^{i}Pr CH_3); 52.8 (d, 3.8 Hz, P—OCH_3); 62.1 (d, 3 Hz, η^2-N=CH); 63.1/65.8 (^{i}Pr CH); 168.1 (σ-N=CH); 194.9 (d, 21 Hz, Ru(P)$(CO)_2$); 200.3 (d, 3 Hz, Ru(P)$(CO)_2$); 198.6/203.3 (Ru$(CO)_2$)
5a	-3.6 (Ru—CH_3); 25.6/26.2 (2×)/28.0 (^{i}Pr CH_3); 64.4/61.3 (^{i}Pr CH); 97.4 (d, 2 Hz, N=CH); 106.6 (N=CH); 128.5 (d, 9.8 Hz, Ph C^3/C^5); 130.5 (Ph C^4); 134.7 (d, 10.8 Hz, Ph C^2/C^6); 135.1 (d, 44.5 Hz, Ph C^1); 200.2/200.9 (Ru$(CO)_2$); 204.8 (d, 22.7 Hz; Ru(P)(CO))
5b	-4.4 (Ru—CH_3); 18.8 (d, 29 Hz, P—CH_3); 22.6 (d, 35.4 Hz, P—CH_3); 25.9/26.7/27.7/28.5 (^{i}Pr CH_3); 64.6/61.4 (^{i}Pr CH); 104.9/98.5 (N=CH); 129.1 (d, 9.5 Hz, Ph C^3/C^5); 130.5 (d, 2 Hz, Ph C^4); 130.8 (d, 10.3 Hz, Ph C^2/C^6); 139.4 (d, 42 Hz, Ph C^1); 201.0/200.5 (Ru$(CO)_2$); 205.7 (d, 21.2 Hz (Ru(P)(CO))
5c	-3.4 (Ru—CH_3); 25.8/26.0/27.6/28.4 (^{i}Pr CH_3); 53.2 (d, 5 Hz, P—OCH_3); 62.8/64.4 (^{i}Pr CH); 100.4 (d, 2 Hz, N=CH); 103.4 (N=CH); 200.4/200.5 (Ru$(CO)_2$); 202.4 (d, 27 Hz, Ru(P)(CO))
6	-11.5 (Ru—CH_3); 22.9/23.1/26.8/27.8 (^{i}Pr CH_3); 61.0/69.5 (^{i}Pr CH); 68.3 (η^2-N=CH); 172.6 (σ-N=CH); 201.7/203.8/206.8/207.6/215.0 (CO)
7	27.6/28.2 (^{i}Pr CH_3); 66.1 (^{i}Pr CH); 109.0 (N=CH); 197.5/197.7 (CO)
8	27.0/25.5 (^{i}Pr CH_3); 49.9 (acetyl CH_3); 63.4 (^{i}Pr CH); 105.6 (N=CH); 197.2/197.6 (CO); 232.8 (acetyl CO)

[a] In $CDCl_3$ solution at 263 K.

are coordinated trans to each other, while the two carbonyl ligands are in a cis position, since the two ^{i}Pr groups of **3e** are equivalent. Additional support was obtained from IR spectroscopic data (vide supra).

Complexes **4a–c** also show the characteristic features of a 6e σ(N)-μ_2(N')-η^2(C=N')-coordinated α-diimine in both the ^{1}H NMR (σ(N)-coordinated imine around 7.5 ppm and η^2(C=N)-coordinated imine around 3.8 ppm) and the ^{13}C NMR spectra (σ(N)-coordinated imine around 170 ppm and η^2(C=N)-coordinated imine around 60 ppm). Furthermore, the carbonyl regions of the ^{13}C NMR spectra show two signals without phosphorus coupling arising from the carbonyls coordinated to Ru2 and two carbonyl signals with different phosphorus couplings arising from the carbonyls coordinated to Ru(1). Since the P–Ru1–C9 and P–Ru1–C10 angles do not differ substantially (98.8 (2) and 88.5 (2)°, respectively), the large difference in coupling constants is probably caused by the differences in bond strengths between the Ru1–C9 bond and the Ru1–C10 bond (vide supra). Finally, it should be noted that no phosphorus coupling could be detected on the proton of the η^2-coordinated imine, not even with *J*-resolved NMR

Scheme IV. Reaction of 2a with CO at Low Temperature and Proposed Structures of the Intermediates X2 and X3

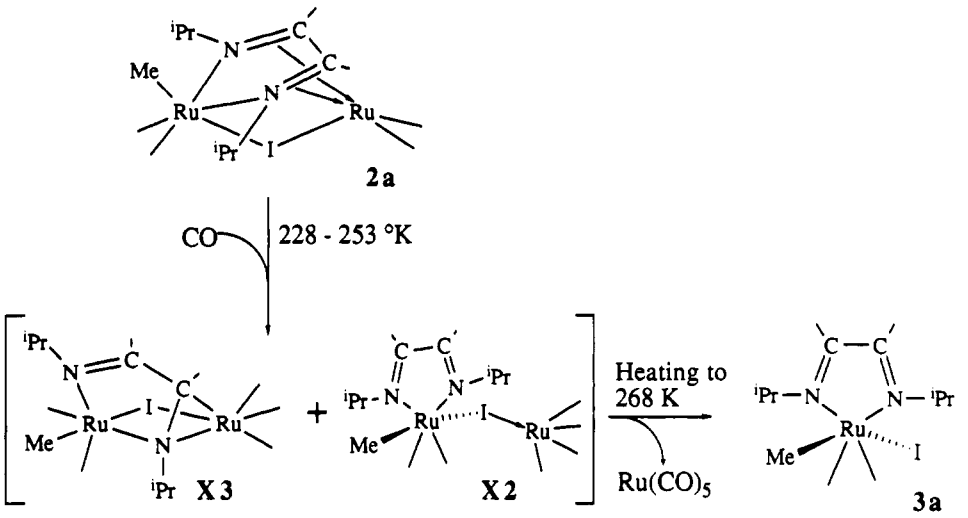

spectroscopy. The phosphorus coupling on the carbon atom of this η^2-coordinated imine moiety is also very small, which is probably due to the cis arrangement of the η^2-bonded imine moiety and the phosphine (P–Ru1–C12 = 108.96 (19)° and due to the relatively weak metal to η^2-(C=N) bond (vide supra).

Both the ^{1}H NMR and the ^{13}C NMR spectra of **5a–c** again show the characteristic features of a DAB ligand in an 8e-donating σ(N)-σ(N′)-η^2(C=N′):η^2(C=N′) coordination mode as discussed for complexes **2a,b** (vide supra). The carbonyl regions of the ^{13}C NMR spectra now show two signals without phosphorus coupling and one signal with phosphorus coupling, which is in agreement with the elimination of the weakly coordinated carbonyl from Ru2 from the complexes **4a–c**. Again, no coupling of the phosphorus nucleus on the two coordinated imine groups is observed in the ^{1}H NMR spectra, whereas the ^{13}C NMR spectra only show a very small coupling on one of the imine carbon atoms (2 Hz) and no coupling on the other imine carbon atom. Since no detailed information of the molecular structure of complexes **5a–c** is available, it is difficult to provide a good explanation for this observation.

In addition to the characteristic features of a DAB ligand in the 6e σ(N)-μ_2(N′)-η^2(C=N′) coordination mode the ^{1}H NMR spectrum of **6** also shows a signal at −16.47 ppm, indicating the presence of a bridging hydride.[51]

The NMR spectroscopic data for complexes **7** and **8** unambiguously show the DAB ligand to be in the 8e-donating σ(N)-σ(N′)-η^2(C=N):η^2(C=N′) coordination mode (imine protons at 6.28 and 6.17 ppm and imine carbons at 109.0 and 105.6 ppm, respectively). Furthermore, the complexes are highly symmetrical and show only two signals for the carbonyl ligands in ^{13}C NMR spectroscopy. From these data we conclude the structure of these complexes to be analogous to the structure of **2a**.

Formation of $Ru_2(Me)(I)(CO)_4$(^{i}Pr-DAB) (2a) and Reaction with CO. $Ru_2(CO)_5$(^{i}Pr-DAB) (**1**) instantaneously reacts with MeI at room temperature with the formation of $Ru_2(Me)(I)(CO)_4$(^{i}Pr-DAB) (**2a**). This reaction may be regarded as an oxidative addition accompanied by a substitution of a carbonyl ligand. In contrast to the oxidative addition of molecular hydrogen to **1**[10] the DAB ligand remains coordinated in a 8e σ(N)-σ(N′)-η^2(C=N):η^2(C=N′) coordination mode (Scheme I).

As reported, **1** reacts with CO to form $Ru_2(CO)_6$(^{i}Pr-DAB) as a result of substitution of a coordinated imine bond.[11,14] As substitution of a coordinated imine bond of the 8e-donating DAB ligand in complex **2a** would lead to a complex with a structure having a 6e-donating DAB ligand, comparable to $H_2Ru_2(CO)_5$(^{i}Pr-DAB),[10] we were prompted to treat **2a** with CO. At room temperature the substitution of a coordinated imine bond indeed occurs, but the reaction does not stop at that stage. It was found that both coordinated imine moieties and the iodide bridge were substituted. As a result, the reaction of **2a** with CO afforded $Ru(Me)(I)(CO)_2$(^{i}Pr-DAB) (**3a**) and $Ru(CO)_5$ (Scheme I). During this reaction three molecules of CO are consumed per molecule of **2a**. Since this reaction is unlikely to proceed in one step, we attempted to detect possible intermediates by monitoring the reaction by means of HP-NMR techniques.

When the reaction mixture was pressurized at room temperature, using a pressure of 10 bar of CO, the mixture turned red during the pressurization time, indicating that the reaction had already started. However, the first NMR spectrum showed that the starting compound **2a** was the major component of the reaction mixture with only a small amount of **3a**. During the course of the reaction the concentration of **2a** gradually decreased while that of **3a** increased. No signals belonging to other compounds could be observed.

When pressurization of the reaction mixture was carried out at low temperature, the mixture remained yellow/orange, indicating that the conversion to **3a** did not take place (or at least was very slow). The sample was then placed into the spectrometer, while the sample space had been precooled to 203 K. The temperature was subsequently raised in 5 K steps, and each time an NMR spectrum was measured 45 min after the new temperature had been reached. At a temperature of 228 K signals for the two unknown complexes **X2** and **X3** appeared. At a temperature of 253 K signals belonging to **3a** appeared, whereas at a temperature of 268 K the species **X2** and **X3** were no longer present and only the signals belonging to **3a** could be observed[52] (Scheme IV).

A complete conversion of **2a** to a mixture of **X2** and **X3** without the formation of **3a** could be obtained by keeping

(51) Values upfield from −15 ppm are usually attributed to bridging hydrides: (a) Reference 10. (b) Moore, D. S.; Robinson, S. D. *Chem. Soc. Rev.* **1983**, *12*, 415.

(52) When the mixture of intermediates **X2** and **X3** is heated to room temperature, besides **3a** also traces of $Ru(C(O)Me)(I)(CO)_2$(^{i}Pr-DAB) are observed, resulting from a carbonylation of the ruthenium–methyl bond. These carbonylation reactions will be subject of a separate paper.[58]

2a under 13 bar of CO at 228 K for about 15 h or under 19 bar of CO at 233 K for about 4.5 h. Monitoring the reaction mixture for longer times showed that intermediates X2 and X3 are stable at temperatures below 253 K and do only react with CO at higher temperatures to yield 3a.[52]

Since both intermediates are observed simultaneously, there is probably only a small difference in thermodynamic stability between X2 and X3. Attempts to detect the presence of an equilibrium between X2 and X3 by means of spin-polarization techniques were not successful. On the basis of the NMR data (Table XII) X3 is believed to contain a DAB ligand in the 6e-donating σ(N)-μ_2(N')-η^2-(C=N') coordination mode, whereas X2 probably possesses a DAB ligand in the 4e-donating σ(N)-σ(N') coordination mode.

Preparation of the Monomeric Complexes Ru(X)(Y)(CO)$_2$(α-diimine). Reaction of Ru(CO)$_3$(α-diimine) (α-diimine = ^{i}Pr-DAB, ^{i}Pr-Pyca)[21] with an oxidative-addition reagent XY (XY = MeI, I_2, benzyl chloride) leads to the formation of Ru(X)(Y)(CO)$_2$(α-diimine) (X = Me, Y = I, α-diimine = ^{i}Pr-DAB (3a); X = Me, Y = I, α-diimine = ^{i}Pr-Pyca (3b); X = Y = I, α-diimine = ^{i}Pr-DAB (3c); X = Y = I, α-diimine = ^{i}Pr-Pyca (3d); X = Cl, Y = benzyl, α-diimine = ^{i}Pr-DAB (3e)) (Scheme II). This reaction therefore appears to be a facile route for the formation of complexes Ru(X)(Y)(CO)$_2$(α-diimine). Complexes 3a[50] and 3c[44] have been reported before, but the synthetic pathway presented here is clearly superior, since the reaction is more facile and gives much higher yields. When the preparation of 3a was performed in heptane instead of hexane, a small amount of Ru(C(O)Me)(I)(CO)$_2$(^{i}Pr-DAB) was formed as well.[53]

A very high yield of 3d was obtained by starting from Ru$_2$(CO)$_4$(^{i}Pr-Pyca)$_2$[12] (Scheme II). In this case the oxidative addition is accompanied by the substitution of the coordinated imine bond. A comparable substitution of a coordinated imine bond has been found for the reaction of Ru$_2$(CO)$_6$(^{i}Pr-DAB) with I_2 (experiment 4(c)ii). In this case Ru(I)$_2$(CO)$_2$(^{i}Pr-DAB) (3c) is produced together with a mixture of Ru$_2$(I)$_4$(CO)$_6$ and Ru$_3$(I)$_6$(CO)$_{12}$.[25]

Since the reaction of Ru$_2$(CO)$_4$(^{i}Pr-Pyca) with I_2 proved to be extremely clean, we attempted to make this route a general one for the formation of complexes Ru(X)(Y)-(CO)$_2$(α-diimine). Unfortunately, the reaction of Ru$_2$-(CO)$_4$(^{i}Pr-Pyca)$_2$ with MeI did not lead to the formation of 3b, probably because MeI is a weaker oxidative agent than I_2. Reactions of Ru$_2$(CO)$_4$(^{i}Pr-DAB)$_2$ with MeI and I_2 were unproductive as well, probably because the η^2-(C=N) to Ru bond strength is higher for R-DAB than for R-Pyca as a result of the better π-accepting ability of the DAB ligand. Furthermore, the greater π-accepting ability of a DAB ligand makes the metal atom less electron rich and therefore less susceptible to oxidative addition.

In the case of I_2 the addition is not performed at the start of the reaction since, in contrast to MeI and benzyl chloride, I_2 reacts with Ru$_3$(CO)$_{12}$ to form several ruthenium halide clusters.[24] The formation of the Ru(CO)$_3$(α-diimine) complexes therefore has to be completed before adding I_2.

A final point to note is that the spectroscopic data indicate a cis arrangement of the two carbonyl ligands in complexes 3 and therefore a trans arrangement for the two new ligands (e.g. R and I (3a,b,e) or I and I (3c,d)). Since oxidative addition results in a cis arrangement of the initial product, the final configuration must be the result of an isomerization. Such isomerizations of octahedral Ru(II) complexes have been reported frequently,[54-57] some of which may be induced by irradiation.[54,55] It has been noted that a trans arrangement of the two iodides or of the iodide and the organic group is the thermodynamically most stable configuration, owing to both steric reasons and/or trans influences.[56,57]

Reaction of Ru$_2$(Me)(I)(CO)$_4$(^{i}Pr-DAB) (2a) with Phosphines. Treatment of 2a with phosphines gave substitution of only one imine bond to yield the complexes Ru$_2$(Me)(I)(CO)$_4$(PR$_3$)(^{i}Pr-DAB) (PR$_3$ = PPh$_3$ (4a), PMe$_2$Ph (4b), P(OMe)$_3$ (4c)) (Scheme I). However, it should be noted that in the case of complexes 4a-c a further substitution by phosphines or carbon monoxide is possible[58] but proceeds with much more difficulty as compared to the system containing no phosphines. Even with a large excess of phosphine, subsequent substitution of the second imine bond and of the iodide bridge are very slow, taking several days to lead to a complete conversion to Ru(Me)(I)(CO)$_2$(^{i}Pr-DAB) and Ru(CO)$_4$(PR$_3$).[59] Heating complexes 4a-c in hexane leads to a recoordination of the substituted imine bond accompanied by an elimination of a carbonyl ligand, thus yielding complexes Ru$_2$(Me)(I)(CO)$_3$(PR$_3$)(^{i}Pr-DAB) (PR$_3$ = PPh$_3$ (5a), PMe$_2$Ph (5b), P(OMe)$_3$ (5c)) (Scheme I). This reaction is reversible, as will be discussed below.

It is of interest to address ourselves to the question why the reaction of 2a with phosphines stops after substitution of one imine bond. A plausible explanation for the stability of complexes 4a-c toward substitution might be the fact that a phosphine causes an increased electron density on the metal, which leads to an increased π donation from the metal to the η^2-coordinated imine group and thus to a stronger Ru-η^2(C=N) bond.[60]

In the reaction of 2a with phosphines the solution instantaneously changed from orange to green upon addition of the phosphine. Subsequently the green color changed within 1 min to yellow in all cases. All attempts to detect an intermediate in this reaction failed. Treatment of 5a-c with CO also led to a similar strongly green colored solution, which again rapidly changed to yellow. IR spectroscopy showed only the absorptions belonging to 4a-c and 5a-c. Although we have not been able to detect any intermediates, the changes in color clearly indicate the involvement of an intermediate in the reaction from 2a to 4a-c and from 5a-c to 4a-c.

A possible reaction sequence is shown in Scheme V together with a proposed tentative structure for the green intermediate X4, which is probably formed by an initial subsitution of the iodide bridge of 2a. Subsequently, a rearrangement gives the thermodynamically most stable product 4a-c, from which 5a-c are formed via loss of CO, probably again via intermediate X4. From complexes 5,

(53) A separate experiment showed that in refluxing heptane 3a slowly reacts with CO to give Ru(C(O)Me)(I)(CO)$_2$(^{i}Pr-DAB).

(54) Jeffrey, J.; Mawby, R. J. *J. Organomet. Chem.* **1972**, *40*, C42.
(55) Barnard, C. F. J.; Daniels, J. A.; Jeffery, J.; Mawby, R. G. *J. Chem. Soc., Dalton Trans.* **1976**, 953.
(56) (a) Barnard, C. F. J.; Daniels, J. A.; Mawby, R. G. *J. Chem. Soc., Dalton Trans.* **1979**, 1331. (b) McCooey, K. M.; Probitts, E. J.; Mawby, R. J. *J. Chem. Soc., Dalton Trans.* **1987**, 1713.
(57) Reichenbach, G.; Cardaci, G.; Bellachioma, G. *J. Chem. Soc., Dalton Trans.* **1982**, 847.
(58) Kraakman, M. J. A.; de Klerk-Engels, B.; de Lange, P. P. M.; Smeets, W. J. J.; Spek, A. L.; Vrieze, K. *Organometallics*, following paper in this issue.
(59) l'Epplattinier, F.; Calderazzo, F. *Inorg. Chem.* **1968**, *7*, 1290.
(60) In this respect it is of interest to mention that complex 2b reacts with carbon monoxide and triphenylphosphine only at high temperatures (refluxing toluene). Since it is known that η^2(C=N) coordination to iron is stronger than to ruthenium,[46,48] this result underscores that the strength of the metal to η^2-imine bond is very important in determining whether a reaction with ligands such as phosphines or CO takes place or not.

Scheme V. Formation and Reversible Interconversion of Complexes 4a–c and 5a–c

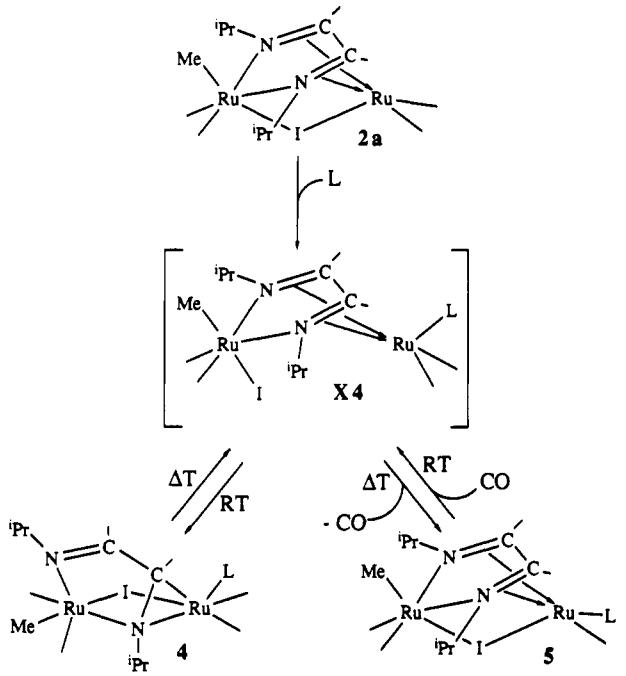

reaction with carbon monoxide leads to complexes **4**, probably also via the proposed intermediate **X4** (Scheme V).

Reaction of Ru(X)(Y)(CO)$_2$(α-diimine) with M(CO)$_4$ Fragments (M = Fe, Ru). Ru(Me)(I)(CO)$_2$(^{i}Pr-DAB) (**3a**) reacts with Ru(CO)$_4$ fragments (prepared from Ru$_3$(CO)$_{12}$) to form Ru$_2$(Me)(I)(CO)$_4$(^{i}Pr-DAB) (**2a**) (Scheme III), showing that the reaction of **2a** with CO is reversible. In the reaction of **3a** with Ru(CO)$_4$ fragments small amounts of Ru$_2$(C(O)Me)(I)(CO)$_4$(^{i}Pr-DAB) (**8**) are formed as a side product.[26] When Ru(CO)$_5$[20] was used as a source for Ru(CO)$_4$ fragments, the dimerization could be performed at room temperature. However, it was found that under these circumstances the trimerization of Ru(CO)$_4$ fragments to form Ru$_3$(CO)$_{12}$ is a serious problem, making the use of excess Ru(CO)$_5$ necessary to obtain a complete conversion to **2a**.

In analogy to the reaction of **3a** with Ru(CO)$_4$ fragments a reaction with Fe(CO)$_4$ fragments (prepared from Fe$_2$(CO)$_9$) was carried out, which afforded the heterodinuclear FeRu(Me)(I)(CO)$_4$(^{i}Pr-DAB) (**2b**) in very high yields with traces of HFeRu(Me)(CO)$_5$(^{i}Pr-DAB) (**6**) as a side product.

Performing this reaction in C_6D_6 afforded a small amount of **6**, which as shown by NMR spectroscopy gave rise to a hydride ligand resonance with normal intensity. The hydride was found to originate from traces of water in the solvent, as was confirmed by performing the reaction in C_6H_6 while 200 μL of D_2O was added. The presence of a deuteride ligand instead of a hydride ligand was confirmed by both ^{1}H NMR and ^{2}H NMR.

Ru(I)$_2$(CO)$_2$(^{i}Pr-DAB) (**3c**) also reacted with Ru(CO)$_4$ fragments to form Ru$_2$(I)$_2$(CO)$_4$(^{i}Pr-DAB) (**7**) (Scheme III). Although **3c** contains two iodide ligands that are capable of bridging a bimetallic unit, **7** only contains one iodide bridge whereas the other iodide is terminally bonded. This observation may be rationalized by considering the trans arrangements of the two halides within **3c**.[44] A bridging coordination of both halides would require a considerable change of geometry in **3c**.

It is interesting to note that in the absence of additional reactants **3c** proved to be very stable in solution. In contrast to the corresponding Fe complex no facile decarbonylation has been observed for **3c**.[61]

The dimerization reactions are shown in Scheme III. In the initial step we propose a coordination of the iodide atom to the unsaturated M(CO)$_4$ fragments, thus leading to intermediates **X2** (compare Scheme IV). Subsequently the two imine groups substitute two carbonyl ligands to form **2a,b** and **7**, respectively. However, in the presence of traces of water the unsaturated species Fe(CO)$_4$ forms a HFe(CO)$_4$-like intermediate which reacts with **3a**/**3c** to give **6**, probably via an intermediate such as **X1** (Scheme III). Support for this mechanism has been found in the reaction of [Ru(CO)$_2$(Me)(^{i}Pr-DAB)][OTf] (prepared by treatment of **3a** with AgOTf) with [HFe(CO)$_4$]$^-$,[62] which also afforded **6** in low yields.

Of interest in this respect is the observation that **6** is only formed in noncoordinating solvents, while the formation of **6** was never observed in solvents such as Et$_2$O and THF, not even when extra water was added. This may be rationalized by the stabilizing effect of coordinating solvents, since the intermediate Fe(CO)$_4$(solvent) will be less reactive toward water than Fe(CO)$_4$ itself, provided the solvent is sufficiently strongly coordinating.

Acknowledgment. We wish to thank Ing. J. M. Ernsting for his advice and practical assistance during the NMR measurements. We wish to thank Mrs. Drs. B. de Klerk-Engels for helpful discussions during the experimental work. We also thank Dr. H.-W. Frühauf and Dr. C. J. Elsevier for suggestions. The X-ray data for **2a** and **4b** were kindly collected by A. J. M. Duisenberg. This work was supported in part (A.L.S., H.K.) by the Netherlands Foundation for Chemical Research (SON), with financial aid from the Netherlands Organization for Scientific Research (NWO).

Supplementary Material Available: Tables of crystal data and refinement details, anisotropic thermal parameters, all H atom parameters, bond lengths, and bond angles and thermal motion ellipsoid plots for **2a**, **4b**, and **6** (19 pages). Ordering information is given on any current masthead page. Listings of observed and calculated structure factors (29, 37, and 27 pages for **2a**, **4b**, and **6**, respectively) can be obtained from A.L.S.

OM9203338

(61) The analogous Fe(I)$_2$(CO)$_2$(^{i}Pr-DAB) easily loses its carbonyl ligands, thermally as well as photochemically, with formation of [Fe(I)$_2$(^{i}Pr-DAB)]$_2$: Breuer, J. Dissertation, Universität Duisberg, Duisberg, Germany, 1989.

(62) Keijsper, J.; van Koten, G.; Mul, J.; Stam, C. H.; Vrieze, K.; Ubbels, H. C. *Organometallics* **1984**, *3*, 1732.